Earthquake Performance of Reinforced Concrete Frames with Different Infill Walls

Hüsnü Coşan

Submitted to the
Institute of Graduate Studies and Research
in partial fulfillment of the requirements for the Degree of

Master of Science
in
Civil Engineering

Eastern Mediterranean University
February 2014
Gazimağusa, North Cyprus

Approval of the Institute of Graduate Studies and Research

———————————————————
Prof. Dr. Elvan Yılmaz
Director

I certify that this thesis satisfies the requirements as a thesis for the degree of Master of Science in Civil Engineering.

———————————————————
Prof. Dr. Özgür Eren
Chair, Department of Civil Engineering

We certify that we have read this thesis and that in our opinion it is fully adequate in scope and quality as a thesis for the degree of Master of Science in Civil Engineering.

———————————————————
Asst. Prof. Dr. Giray Özay
Supervisor

Examining Committee

———————————————————

1. Asst. Prof. Dr. Giray Özay   ———————————————————

2. Asst. Prof. Dr. Alireza Rezaei   ———————————————————

3. Asst. Prof. Dr. Serhan Şensoy   ———————————————————

ABSTRACT

Infill walls are used frequently as interior or exterior partitions in reinforced concrete frames in the world. The behavior of infill wall frames have been studied experimentally and analytically by a number of researchers and it has been recognized that infill walls have important effects on dynamic characteristics of structural system. However, these effects of infill walls neglected in analysis of buildings. For this reason, the horizontal rigidity effect of infill walls has not been proven to be a valid model. Therefore, infill walls generally defined as dead load in the analysis to stay on the safe side but ignoring the infill panel interaction is not always on the safe side under lateral loads. It may adversely affect the structural system during an earthquake.

The main purpose of this study is the effects of infill walls on the structural behavior which are not accounted in the structural design of reinforced concrete buildings. For this purpose, nonlinear analyzes were performed using dissimilar modeling methods proposed by different researchers. These methods were analyzed using different analyze softwares. Three separate building systems were used for each different method. Hence, diverse building models have been created and the behaviors of these structures under lateral loads have been investigated in order to identify the effects of infill walls.

Each building model created was analyzed in three different situations including bare frame, the frame with brick infill wall and the frame with Autoclaved Aerated

Concrete (AAC) infill wall. Hereby, the outcomes obtained from analysis on bare frame and the frame with infill walls has been compared.

At the end of the analysis, it is observed that infill walls have significant effect on structural period, lateral displacement, base shear force and structural behavior.

Keywords: Infill wall, structural period, lateral displacement, base shear force, earthquake

ÖZ

Dünyada bölme duvarlar, betonarme çerçeve sistemlerde iç ve dış elemanlar olarak sıklıkla kullanılmaktadır. Birçok araştırmacı dolgu duvarlı çerçeveler üzerinde deneysel ve analitik olarak çalışma yapmış ve dolgu duvarların yapı sisteminin dinamik özellikleri üzerinde önemli etkilere sahip olduğunu kabul etmişlerdir. Ancak dolgu duvarların bu etkileri bina analizlerinde ihmal edilmektedir. Bunun nedeni, dolgu duvarların yatay dayanıma olan etkisinin halen kanıtlanmış geçerli bir modeli olmamasıdır. Bu nedenle, analizlerde dolgu duvarlar genellikle güvenli tarafta kalabilmek için ölü yük olarak tanımlanmaktadır. Fakat dolgu paneli etkileşiminin göz ardı edilmesi yatay yükler altında her zaman güvenli değildir. Deprem esnasında yapı sistemine olumsuz etkileri olabilir.

Bu çalışmanın amacı, betonarme yapı tasarımında hesaba katılmayan bölme duvarların yapı davranışı üzerindeki etkileridir. Bu amaç için farklı araştırmacıların dolgu duvarlar için önerilen farklı modelleme metotları kullanılarak analizler gerçekleştirilmiştir. Bu farklı modelleme metotlarının analizleri farklı analiz programları kullanılarak yapılmıştır. Her farklı modelleme tekniği için üç farklı bina sistemi kullanılmıştır. Farklı model yapılar oluşturulmuş ve dolgu duvarların etkisini belirlemek amacıyla bu yapıların yatay yükler altındaki davranışları incelenmiştir.

Her yapı modeli boş çerçeve, tuğla dolgu duvarlı ve gazbeton dolgu duvarlı çerçeve olacak şekilde oluşturulmuş ve üç farklı durumlarda analiz edilmiştir. Böylelikle dolgu duvarlar boş çerçeve ve dolgu duvarlı çerçeve analizlerinden elde edilen sonuçlarla karşılaştırılmıştır.

Analizler sonunda, dolgu duvarların periyot, yanal deplasman, taban kesme kuvveti ve yapı davranışı üzerinde önemli bir etkiye sahip olduğu gözlemlenmiştir.

Anahtar kelimeler: Dolgu duvar, periyot, yanal deplasman, taban kesme kuvveti, deprem

To My Family

ACKNOWLEDGMENTS

I would like to express my deepest gratitude to my supervisor Asst. Prof. Dr. Giray Özay for their support and encouragement during this study. It is an honor for me to have worked with him.

I also would like to thank Assoc. Prof. Dr. Umut Türker for his invaluable suggestion and supports since my undergraduate education.

Finally, I would like to present my deepest thanks to my family for their support and encouragements throughout all my life.

TABLE OF CONTENTS

LIST OF TABLES

LIST OF FIGURES

LIST OF SYMBOLS

A_m Area of strut

A_2 Residual Area of the strut

b_w Compression struts width

E_{infill} Approximate modulus of elasticity of infill wall

E_m Expected modulus of elasticity of infill material

E_f Young's modulus

f_c Infill wall compressive strength

$f_{m\theta}$ Compressive strength of infill wall

f_t Tensile strength of infill wall

h   Column height between centerlines of beams

h_z Distance between struts

h_w Height of infill panel

p_i Incremental load value of SeismoStruct

p_0 Nominal value defined previously in SeismoStruct

t_w Thickness of infill panel

l_w Length of infill panel

z   The contact length of the strut

x_{oi} Horizontal offset

y_{oi} Vertical offset

w   Equivalent diagonal compression strut width

λ The dimensionless relative stiffness factor

λ_i Load factor of Seismostruct

$E_c I_c$ Bending stiffness of the columns

I	Moment of inertia of the surrounding frame member
θ	Angle between the infill diagonal and the horizontal
ε_m	Strain at max stress
ε_u	Ultimate strain
ε_{cl}	Closing strain
τ_o	Bond shear strength
τ_{max}	Maximum shear stress
μ	Coefficient of friction

LIST OF ABBREVIATIONS

AAC   Autoclaved Aerated Concrete

ATC   Applied Technology Council

FEMA   Federal Emergency Management Agency

B   Yield State

IO   Immediate Occupancy

LS   Life Safety

CP   Collapse Prevention

C   Ultimate State

Chapter 1

INTRODUCTION

1.1 General

In the 21st century engineering plays a more vital role in our lives than ever before. The world is forever growing and evolving. The technology is also growing with new structures in the world, as is the demand for new buildings and good infrastructure. Therefore, modern life is almost wholly dependent on engineering.

As a result of technological advances, experiments and researches on earthquake engineering have enabled this field to reach a further point. Therefore, the design methods based on performance are being improved day by day. Engineers can determine the behavior of a building at an event of an earthquake or enable the building to behave in a certain way by using probability methods.

However, today, for the analysis and designs based on performance, especially for the reinforced concrete structures, outer walls and inner partition walls between the frames are considered as non load bearing elements. These walls are only defined as dead loads over the beams and the analysis and designs are implemented in accordance with this.

As a result of this approach, the structural period, earthquake load transferred to each column and beam, potential short column mechanism and the potential mode of failure under earthquake load is not assessed correctly (Sevil et al., 2010).

Investigations after important earthquakes and empirical studies by several researchers show that the infill walls are considerably effective on horizontal rigidity and strengths and on the horizontal load bearing capacities of the buildings.

Recent empirical studies have observed that the structural analysis implemented with partition walls which are not modeled in an unconsidered or unrealistic way would not reflect the truth and would not provide correct outcomes (Sevil et al., 2010).

However since there is no reliable calculation method considering the contribution of partition walls and because these calculation methods which would reflect this contribution to the model are different and complicated, the infill walls are ignored in the calculations (Kızıloğlu, 2006).

On the other hand the infill walls add an additional rigidity to the frame and mostly decrease the structural period and becomes effective in the force distribution of the structure. As a result of the damage on infill walls, the energy would be decreased to an extent during an earthquake.

Earthquake codes in many countries have neglected the effects of infill walls beside load bearing system elements. At the end of empirical and analytical studies by several researchers, various modeling methods on infill walls are suggested.

1.2 Problem Statement

Behavior of infill walls on seismic performance of reinforced concrete building is an intricate issue since their exact role in the seismic load resistance is not yet completely understood. Because of infill walls are composite material, especially infill materials and workmanship are variable factors.

Infill walls with columns and beams of the frame interfaces movement is provide structural damping. Infill and frame separation and cracks on infill walls enhances the structural damping further. These are consuming a significant amount of seismic energy. For all these to occur, the infill wall properties and behaviors should be better understanding and it is necessary to design structures according to this. If this is done unconsciously, dynamic properties of structural system may change during an earthquake. But unfortunately, there is no any certain standard of infill walls and it is very difficult to determine all of them in the analysis phase.

1.3 Objective and Scope

The first moment of the earthquake, infill walls are acting as shear wall, afterward because of less resistance than the frame elements, infills are cracking and remains disabled, after a few seconds it is known that there is no effect on structure.

Unfortunately today, positive and negative effects of infill walls on structural building analysis are not well known. Therefore, especially horizontal load effects of these walls are assumed to be the non bearing element.

In this study, two different infill wall materials used and the results were compared. Moreover, dissimilar modeling methods were mentioned in detail to observe the behavior effects of infill walls on the structure. Different building systems have been created for the dissimilar modeling methods and the behavior of systems were observed under lateral loads. All analyzes were made in the SeismoStruct and Sap2000 nonlinear analyze softwares for these diverse modeling methods.

1.4 An Overview on the Chapters

This thesis consists of 8 chapters. Chapter 1 gives an overview about the infill walls and describes the objective and scope of the study. Chapter 2 concentrates on some of the previous studies and focuses on the topics which researchers mentioned frequently. Chapter 3 focuses on the behavior of Autoclaved Aerated Concrete (AAC) infill wall and brick infill wall materials under diagonal pressure. Chapter 4 generally describes the modeling technique suggested by Crisafulli (1997) and in chapter 5, using this modeling technique, different building systems were analyzed with SeismoStruct analyze software. Chapter 6 gives information of modeling techniques recommended by Asteris (2003) and in chapter 7, using this modeling technique, existing building systems were modeled and analyzed with Sap2000 analyze software. Finally, chapter 8 is conclusion section which gives the general information regarding studies and the analysis results.

Chapter 2

BEHAVIOR OF INFILL WALLS IN REINFORCED CONCRETE STRUCTURES UNDER HORIZONTAL LOAD

2.1 Literature Review

The effect of infill walls and infill wall frames on structural system has been the subject of various empirical and analytical studies. Important advances for reinforced concrete frames have been recorded.

The first study which shows the interaction between infill walls and frames has been done by Polyakov in 1956. In this study it has been stated that infill walls behave as a cross coupling on the frame with equivalent compression strut (Karslıoğlu, 2005).

Studies on infill wall frames in 1960 have carried out experiments in order to be able to predict the lateral strength and rigidity of the infill wall frame structures. At the end of these experiments, it has been found out that infill walls behave as the equivalent compression struts which is still being used for modeling today (Bounopane & White, 1999). A relationship between the width of these equivalent compression struts and vertical and horizontal contact length has been obtained (Hendry, 1981).

Merhabi et al., (1996) have carried out experiments on frames with brick infill and frames with open brick infill and determined that with an increase in the vertical load

on infill walls, there can be up to 25% increase in the total horizontal load bearing capacity of the composite frame.

According to the study on reinforced concrete frames both with and without infill walls, Altin et al., (1992) have stated that the frame rigidity and system strength will increase significantly if a proper relation is obtained between infill wall and the frames.

The results stating that the contact surface of infill and its surrounding frame plays an important role on the horizontal rigidity and strength of infill wall frames have been revealed (Stafford, 1962, 1966).

Liauw and Kwan (1984) have used nonlinear finite elements to determine the modes of failure and the equivalent strengths according to the plastic theory they have developed for single and multi storey frames. As a result, it has been found out that the bending strength of the frame is the most important parameter and the empirical and analytical studies have been accommodated.

Grovidan et al., (1986) have carried out empirical studies on two separate systems both 7 storied, one with bare frame and one with infill wall frame, both under loads and they compared the horizontal rigidities, ductility and energy absorption capacities of these structures. At the end of this study, it has been observed that infill wall frames have greater base shear comparing to simple frames.

Dowrick (1987) has observed that infill walls increase the structural strength and rigidity and Bayulke (2003) has stated that infill walls decrease the structural periods as well as increasing system rigidity.

Celep and Gencoglu (2003) have investigated buildings with different modulus of elasticity and different wall cross sectional area on exemplary structure. On the exemplary structure, they have connected infill walls to the frame in three different methods and they have found out the periods of the exemplary structure for each case. Based on the obtained outcomes, they have observed that the infill walls are effective on the rigidity and periods of the structure. Additionally, they have stated that even small amounts of infill walls have significant effects on the rigidity and period of the building and that greater the modulus of elasticity of the wall, greater the horizontal displacement rigidity of the structure.

Budak (2006) has modeled a frame in order to determine the effects of infill walls. This model has been compared with the three different thicknesses of infill walls and simple frame. This case has been analyzed according to two different soil types, two different wall densities and two different wall modulus of elasticity. At the end of this analysis, it has been recorded that the existence of infill walls affects the structural period significantly. Increasing the earthquake load to an extend depending on the modulus of elasticity decrease of the walls with different modulus of elasticity and does not affect the structural period of the change in infill wall thickness significantly.

Baran (2012) has done some experiments in order to observe the influence of infill wall frame. He has experimented with a 1/3 scale, single span and two-storey

reinforced concrete frames. Common frame deficiencies are reflected in the structure deliberately. These deficiencies are low concrete strength, use a flat reinforcement, insufficient overlap between floors of longitudinal reinforcement length and the combination of weak column-strong beam. He has observed that lateral load carrying capacity of brick infill wall frame is approximately 3.5 times higher than the simple frame.

Jadhao and Pajgade (2013) have investigated seismic behavior of multi-story buildings under earthquake loads to observe the effects of infill walls. At the end of the analysis, they compared the performance of frame with full infill and bare frame. They have observed that the performance of frame with conventional clay bricks and AAC infill wall models were significantly greater than bare frame.

2.2 Effect of Infill Walls on Structural Behavior

Several studies based on empirical and theoretical researches have revealed that infill walls have effects on structural behavior. However, today, these walls are being considered as static load on structure or vertical load in structural analysis, because they are generally being used to divide the building into parts architecturally.

Reinforced concrete frames with infill walls are widely used building types in various countries. The infill wall damage on the reinforced concrete frames holds an important part of the material loss caused by the earthquake. During the shaking of the ground, the collapse of the infill walls as a whole or as a part influences the horizontal load strength of the reinforced concrete frames and the earthquake performance, to an extent where it determines the building to remain standing or destroy in some cases. The observations after the last earthquake in Van, Turkey

(October, 2011), show that infill walls had contributed the strength of the buildings which remained standing (Yakut et al., 2013).

The contribution of infill walls on reinforced concrete building is related to the relative strength of infill wall and reinforced concrete frame, the quality of workmanship of the infill wall and the connection of the infill wall and the frame surrounding it. During the earthquake in Van (Figure 2.1. a, b, c) infill walls had a significant contribution on the strength and enabled the building to remain standing in some cases. However, in some other cases, the infill walls had been decomposed from the system because of in and out of plane solicitation (Figure 2.1. d) (Yakut et al., 2013).
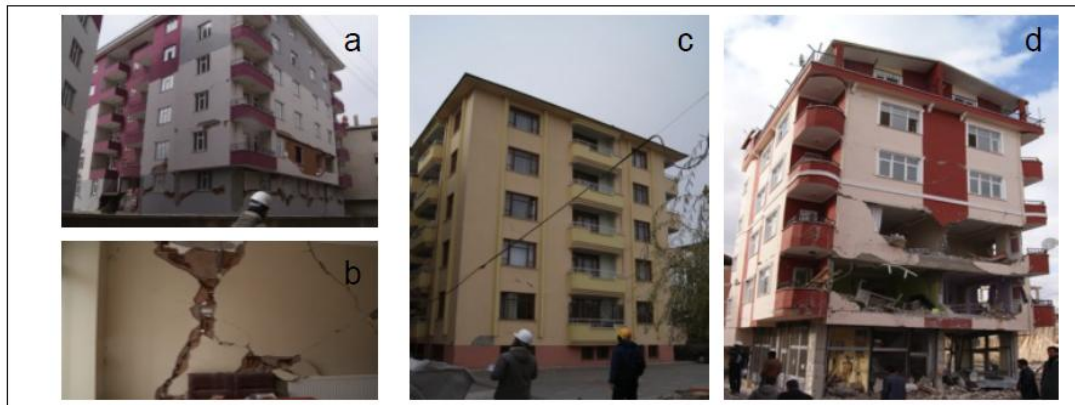
Figure 2.1 Infill Wall Damages Observed After the Earthquake in Van, 2011 a) in Plane Damage, b) Interior Wall Damage, c) Moderate Damage, d) Heavy Damage of the Inner and Outer Plane (Yakut et al., 2013).

The traditional designs of reinforced concrete buildings do not include infill walls as their contribution on the horizontal load strength. This tendency would be considered as true if the infill walls were separated from the frame. However, the practice of construction is not in this way. This separation could be used by leaving a gap between the infill walls and the frames by preventing them from damaging each

other during the earthquake. However, the practice of construction is by placing the infill walls inside the frames and attaching them on the frame by mortar after the reinforced concrete frames are completed (Yakut et al., 2013).

Studies and observations after the various earthquakes show that the infill walls have more rigidity contribution than mass contribution. Many researchers in the world have stated that infill walls increase the rigidity of a structure and beside this feature, they increase energy absorption capacity and damping capacity, and also decrease the structural period. Generally, infill walls influence the load bearing capacity, rigidity, ductility and energy absorption capacity of a structure (Yıldırım, 2009).

2.2.1 Load Bearing Capacity

Infill walls affect the horizontal load bearing capacity of a structure. It has been observed that the horizontal load bearing capacity of a composite structure with infill walls is 1.5 times more than a reinforced concrete structure (Negro & Verzeletti, 1996).

Infill walls restrict the displacement of a structure like shear walls. This restriction distinguishes from shear walls in terms of being valid at the beginning of an earthquake or during a low intensity earthquake. Dowrick (1987) has revealed that the infill walls affect the load bearing capacity of a structure.

Grovidan et al., (1987) have carried out experiments on models of single span and 7 storey reinforced concrete and found out that infill wall frames have two times more load bearing capacity than simple frames.

Merhabi et al., (1996) who have carried out studies on composite frames have investigated different infill wall systems with bricks and hollow bricks. In these studies they have concluded that hollow brick wall frame has 2.1 times more horizontal load bearing capacity than simple frame and brick wall frame has 3.2 times more horizontal load bearing capacity than simple frame.

2.2.2 Rigidity

Dowrick (1987) have stated in his study that infill walls increase the rigidity of a structure and change the rigidity distribution of a structure in horizontal and vertical directions.

Brokken and Bertero (1981) have studied on 18 different models under loads expressing the earthquake behavior. Investigations they have carried on using four different infill materials and they have observed that the infill walls affect rigidity significantly.

Negro and Verzeletti (1996) have compared the maximum displacements on the top floor of the frames and have observed that the maximum displacement occurred at an infill wall frame is 2.6 times less than a simple frame. Also it has been observed that infill wall frames have higher rigidity under horizontal loads than simple frames.

2.2.3 Ductility

Ductility is the ability of a structure, an element of a structure or a cross section to be able to create a massive deformation without any significant reduction in the bearing capacity.

Grovidan et al., (1987) have compared ductility of simple frame and infill wall frame systems and have concluded that a simple frame has more ductile. The ductility of simple frames is 3.29 times more than the infill wall frames. It shows that infill walls reduce the level of ductility of the building system according to the simple frame.

2.2.4 Energy Absorption Feature

Energy absorption capacity is defined as the area under curves in a load-displacement diagram during the loading applied on the system.

Dowrick (1987) have observed that the infill walls increase the energy absorption capacity of a structure significantly.

Grovidan et al., (1987) have determined that infill wall frames have more energy absorption amounts than simple frames.

2.3 Failure Mechanisms of Infill Walls under Lateral Loading

Researches and experiments have shown that infill wall frames can create several failure mechanisms depending on the strength and stiffness of the bare frames and infills with geometric configuration of the framing system. According to experimental observations, infill walls of the frame can classify five main failure mechanisms (Merhabi et al., 1994) (Figure 2.2).
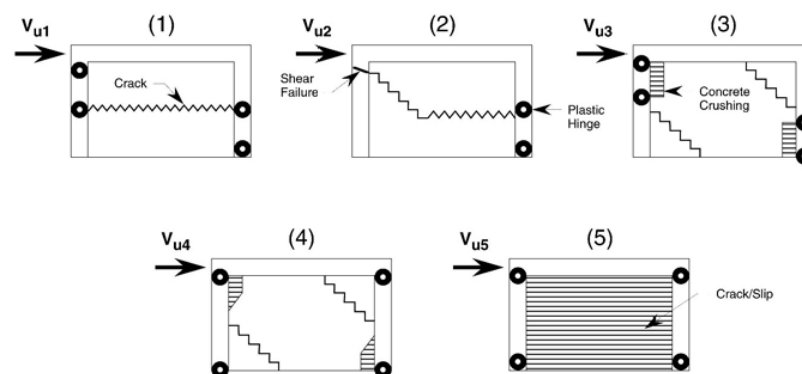
Figure 2.2 Various Failure Mechanisms (Merhabi et al., 1994)

The failure mechanism of an infill wall frame is dependent on the strength and stiffness of infill and bare frame. Therefore, strength and stiffness are very important parameters for infill walls according to the bare frame under lateral loads. A comparatively weak infill is most desirable. Additionally, the strength of the mortar joints is also one of the most important criteria (Merhabi et al., 1994).

Failure mechanism 1 in Figure 2.2 corresponds to horizontal sliding failure of the infill at mid-point. In this case the lateral resistance is the sum of the shear forces in the columns and the residual shear resistance of the wall. The resistance of the frame is governed by the hinges formed at one end and the mid-height of each column.

In failure mechanism 2, the shear failure develops at one or more locations in the columns. This was a brittle mechanism associated with a significant drop of the load carrying capacity and it normally occurred in nonductile frames with strong infills.

In third mechanism, masonry reaches the crushing strength along the wall to frame interface and plastic hinges develop near the beam-to-column joints.

In forth mechanism, infill reaches its compressive strength at corners and plastic hinges are formed at both ends of the column. This mechanism has strong frame. Therefore mechanism characterized by infill corner crushing. The wall-to-column interface has a parabolic distribution along the contact length.

Finally, fifth mechanism occurs in a strong infill bounded by a relatively strong and ductile RC frame.

2.4 Modeling of Infilled Frame

Behavior of infill wall frames under lateral loads have been examined by many researchers. Researchers have two different approaches in relation to infill walls to be reflected in the analytical model. First one is micro modeling where each wall panel is represented by a finite element mesh. The second approach is macro modeling. It is based on behavior of the infill walls reflected on physical model. Micro modeling is difficult to implementing large building systems. Therefore, macro modeling approach is adopted more widely.

Chapter 3

COMPRESSION STRENGTH OF INFILL WALL MATERIALS

This chapter has two dissimilar experiments performed by different researches to identify the modulus of elasticity and compressive strength of brick and AAC infills. Experiment result values used in performance analysis of buildings.

3.1 Brick Wall Compressive Strength

Infill wall compressive strength, f_c , found by testing according to one of the diagonals of the plastered hollow brick infill elements with the applied compression. In the experiments specifically produced hollow bricks (Figure 3.1) were used. For mortar and plaster, low compressive strength mortar and plaster were used in order to reflect the simple workmanship in the application. The non plastered and plastered hollow brick infill walls which have the same characteristics and with the sizes of 700 mm x 700 mm prepared in the Structural Mechanic Laboratory of Middle East Technical University were tested with the applied compression in accordance with one of the diagonals (Sevil, 2010). For the non plastered hollow brick infill, the approximate compressive strength was f_c, 3.5 MPa, the approximate modulus of elasticity was E_{infill} , 5000 MPa and for the plastered hollow brick infill these values were 4.5 MPa and 7000 MPa, respectively. The experimental set up is shown in Figure 3.2 (Sevil et al., 2010).
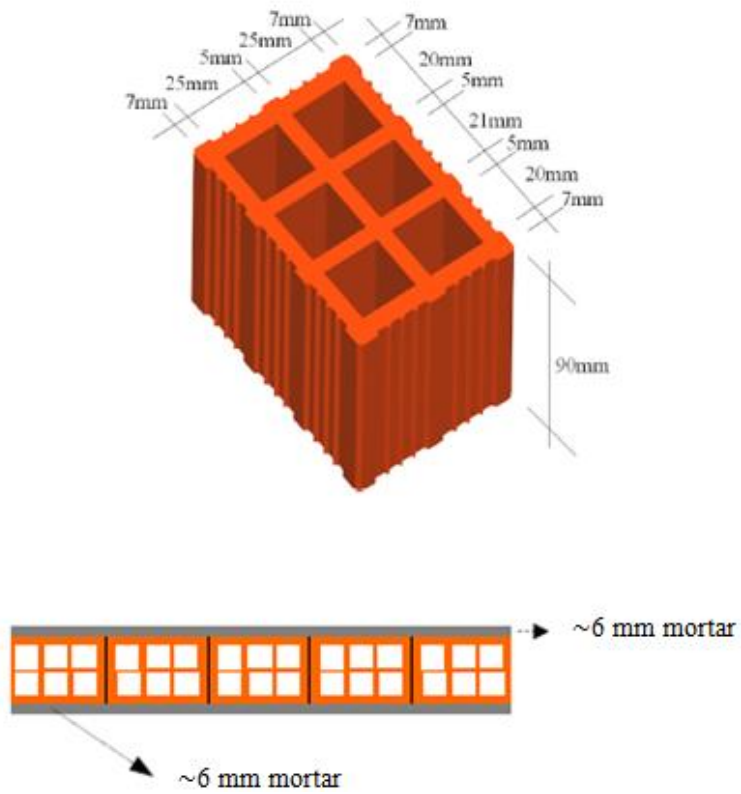
Figure 3.1 Hollow Brick and Walling Used in the Experiments (Sevil et al., 2010)
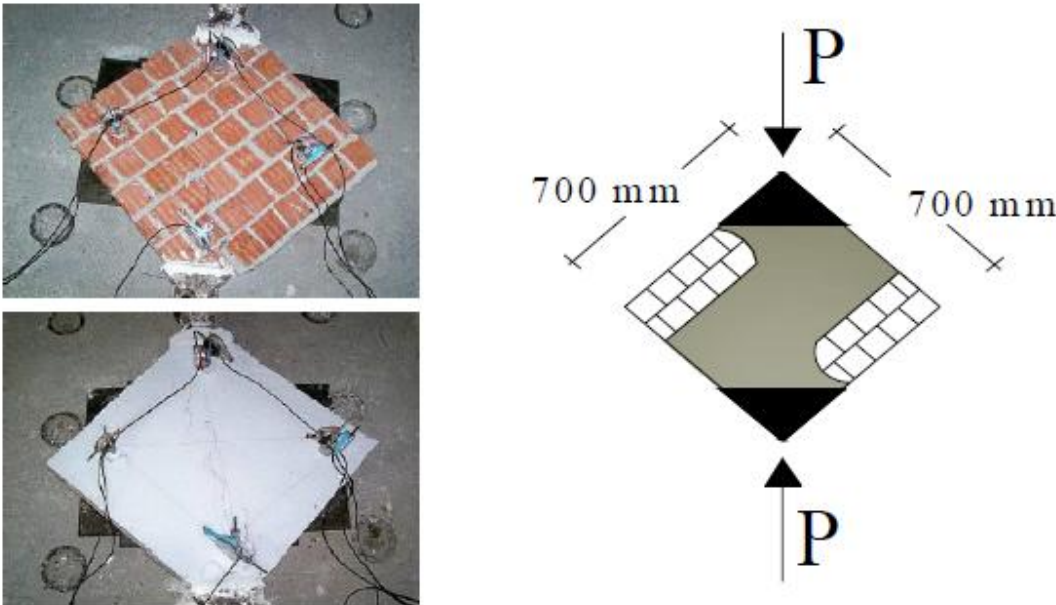
Figure 3.2 Experimental Set Up for Hollow Brick Infill (Sevil et al., 2010)

3.2 Autoclaved Aerated Concrete (AAC) Wall Compressive Strength

In this study the compressive strength and modulus of elasticity of the AAC walls were investigated experimentally by using common mortars and AAC masonry glue. The experiments were held in the Structural Mechanic Laboratory of Middle East Technical University (Alakoç et al., 1999).

In the compression experiments AAC materials within the classification of G4/06 strength were used. The sizes of experiment elements were 125x120x20 cm as shown in Figure 3.3. In this experiment series, a total of 15 AAC wall elements were tested under diagonal compression and for each element there were 3 different mortars (B, C and T). For each mortar type 5 AAC wall elements were used. Mortar components are given in Table 3.1 and the experimental set up is shown in Figure 3.4.
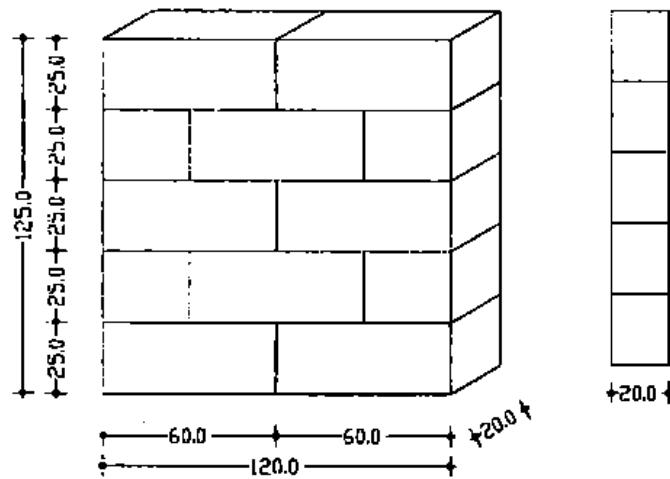
Figure 3.3 Wall Experiment Elements (Alakoç et al., 1999)

Table 3.1 in volume mixture proportions of mortar types

Type of Mortar	Sand	Cement	Lime slurry	Lime
B	4	1	-	1/2
C	5	1	1	-
T	AAC block masonry glue			
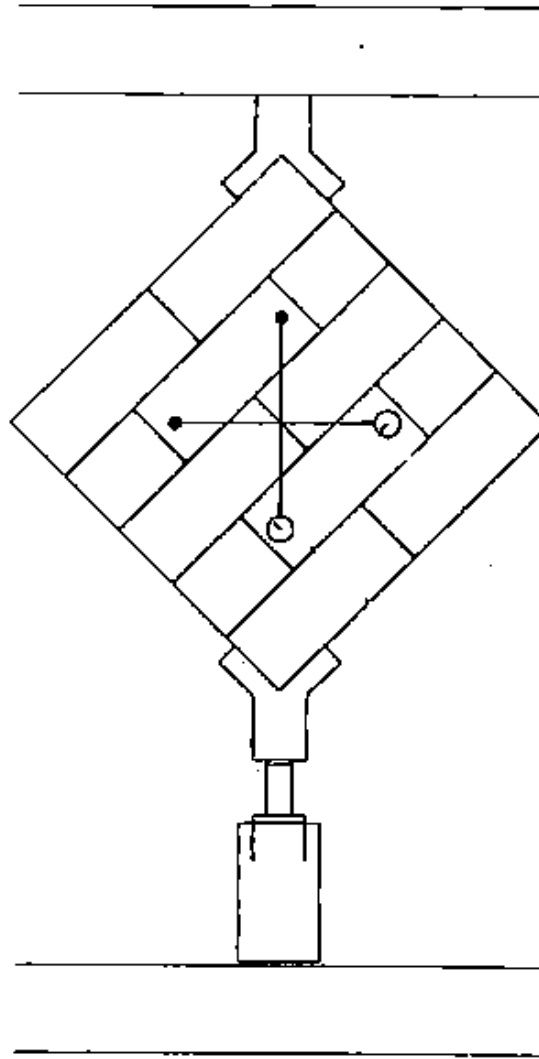
Figure 3.4 Experimental Set Up of Wall Experiments (Alakoç et al., 1999)

According to the results obtained from the experiment elements, it has been found that the strengths of the samples walling with T type mortars was approximately two times more than the samples walling with B type mortar and 1.15 times more than the samples walling with C type mortar. The results of the experiment are given in Table 3.2.

Table 3.2 Diagonal breaking loads

B type mortar	C type mortar	T type mortar
62.98 kN	108.18 kN	122.55 kN

It has been observed that the diagonal cracking has occurred in the experimental elements walling with T type mortar with AAC material and that the failure has occurred in the elements walling with B and C type mortars along the joints. Approximate diagonal load – diagonal displacement graph of the elements walling with B, C and T type mortars is given in Figure 3.5.
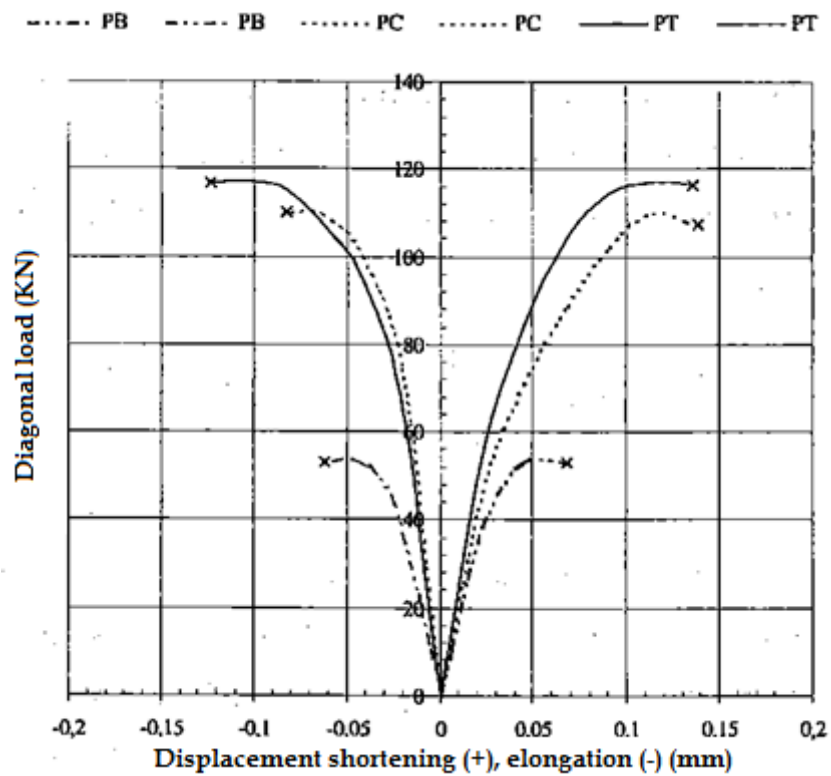
Figure 3.5 Diagonal Load – Diagonal Displacement Graph (Alakoç et al., 1999)

As a result it has been observed that T type mortar increases the wall compressive strength to some extend compared to widespread mortars. The approximate compressive strength, f_c, was found as 4.322 MPa, the approximate modulus of elasticity, E_{infill}, was found as 2728 MPa in the experiments prepared with T type mortar (~2 mm).

Chapter 4

DOUBLE STRUT MODEL

4.1 Element Model Formulation

4.1.1 Equivalent Strut Approach

The model illustrates the equivalent strut approach as a multi-strut formulation where the aim is to show how the surrounding frame is influenced by the masonry panel (Smyrou, 2006).

Crisafulli (1997) has studied on the single strut model limitations. It seems to be the simplest rational illustration which is used for the analysis of infilled frames. He also has investigated how various multi-strut models affect the structural response of infill frames. These focused on degree of stiffness of the building and the behaviors caused in the surrounding frame.

Figure 4.1 illustrates the numerical outcomes found out for the three different strut models. The aim was to compare these outcomes with the equivalent finite element model.

During the analysis, the strut area was maintained constant, the static lateral load was applied and the linear elastic behavior was predicted however the nonlinear influences were assumed to describe the infill panel-frame interface is separated in the finite element models.
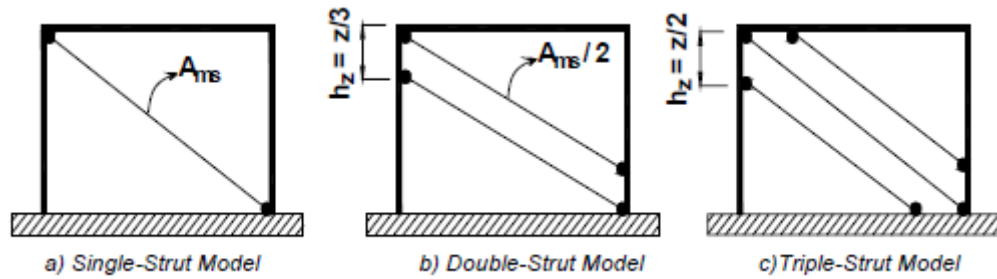
Figure 4.1 Modified Strut Models (Crisafulli, 1997)

According to the outcomes obtained, the cases studied have similar infill frames stiffness. The double and triple-strut models are also considered to have minimum reduction of stiffness. The one worth noting is the triple-strut model where the stiffness would vary considerably; this variation is generally based on the distance between struts h_z. The increase in the distance h_z can be assessed as a fraction of the contact length. This enables a decrease in the stiffness and the control is generally supplied by the mechanical properties of the columns (Smyrou, 2006).

Moreover, the bending moments were undervalued by the single-strut model. Larger values were obtained from the double-strut model and a greater similarity has been established from the triple-strut model even though there are some exceptions at the end of the columns. Correlative outcomes were obtained for the shear forces as well. Lastly, the axial forces at highest levels in concrete members were almost identical in all models (Smyrou, 2006).

The outcomes have showed that even though the simplicity of the single-strut model propose a sufficient evaluation for the infill frame stiffness and the axial forces generated in the frame members by the lateral loads. Yet, in order to reach realistic values for the bending moments and the shear forces of the surrounding frame, a relatively refined model is vital (Smyrou, 2006).

Even though the construction of an adequate tool by the single-strut model for the estimation of the total response and the triple-strut model exceeds in detail, Crisafulli (1997) illustrated the double-strut model approach as fairly definite and limited entangled (Smyrou, 2006).

On the other hand, the model presented shows the struts that are not clearly linked to the frame. Precise explanation and structure of the model is given in the following section.

4.1.2 Explanation of the Model

The model given is made up of four-node masonry panel elements and is designed to illustrate the behavior of framed structure infill panels. Each of these panels is illustrated by five strut members, two parallel struts in each direction diagonally (Figure 4.2) and single strut as two opposite corners diagonally in order to bear the shear from top part to the bottom part of the panel (Figure 4.3). The final strut operates across the diagonal. This can be compressed so it links the separate top and bottom corners based on the deformation of the panel.
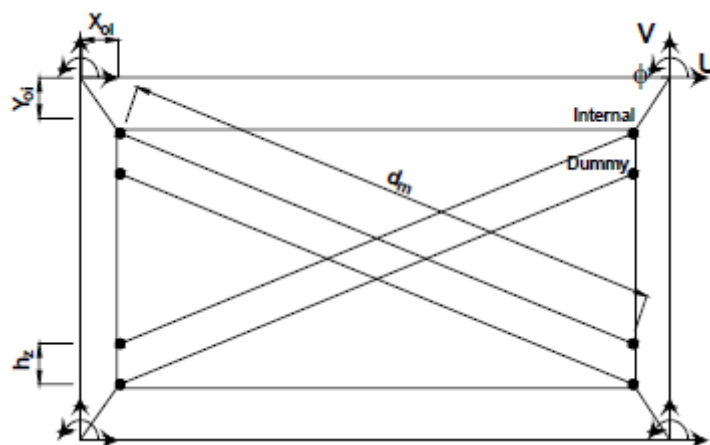
Figure 4.2 Infill Panel Element Configuration (Crisafulli et al., 2000)

The first four struts apply the masonry strut hysteresis model. This model was studied and put into use by Crisafulli et al., (2000). On the other hand, shear strut applies a bilinear hysteresis rule. Shear modeling, using a shear spring on both sides of load can be seen on the Figure 4.3.
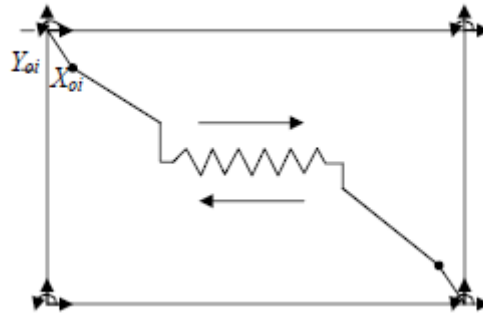
Figure 4.3 Shear Spring Modeling (SeismoSoft, 2013)

4.1.3 Separation Between Struts Vertically

When there is separation between struts vertically, h_z causes plausible outcomes. These outcomes are 1/3 and 1/2 of the contact length. The contact length z, was explained by Stafford (1966). As a result, it has been found out that the dimensionless relative stiffness parameter λ, has a value of

$$z = \frac{\pi}{2\lambda} \tag{4.1}$$

Where

$$\lambda = \sqrt[4]{\frac{E_m t_w \sin(2\theta)}{4 E_c I_c h_w}} \tag{4.2}$$

23

$E_c I_c$ is defined as the bending stiffness of the columns, E_m is modulus of elasticity of infill wall material, t_w is infill panel thickness, θ is angle between the infill diagonal and the horizontal, h_w is height of infill panel and also the parameters are given in Figure 4.4.
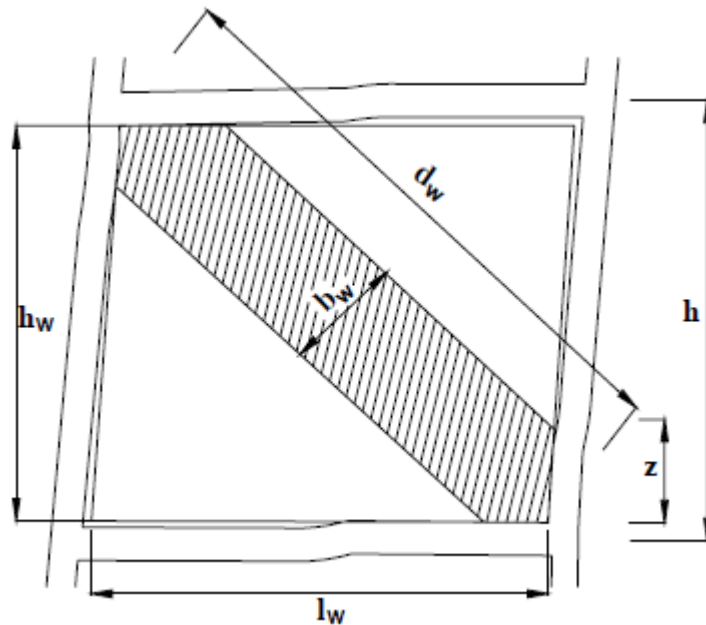
Figure 4.4 Configuration with the Geometrical Properties of Infill Panel (Smyrou, 2006)

Where h is the column height between centerlines of beams, l_w is length of infill panel, d_w is diagonal length of infill panel and b_w is the compression struts width.

4.1.4 The Area of Strut

A_m is given for the area of strut. The area of strut can be explained as the product of the panel thickness. The equivalent strut width is shown as b_w. It can show changes from 10% to 25% in the diagonal of the infill panel, which forms the conclusion of the study by Stafford (1962) based on empirical data and analytical outcomes. Several empirical expressions can also be found by various researchers who evaluate the equivalent width, shown hereafter.

Holmes (1961) suggested that

$$b_w = d_w/3 \qquad (4.3)$$

Mainstone (1971) has established a group of equations for each performance level of Equation (4.4).

$$b_w = 0.16\lambda_h{}^{-0.3}d_w \qquad (4.4)$$

Equation (4.5) was used by Klingner and Bertero (1978). This equation was also offered by Mainstone and Weeks (1970) earlier.

$$b_w = 0.175(\lambda h)^{-0.4}d_w \qquad (4.5)$$

Equation (4.6) was introduced by Liauw and Kwan (1984). They have taken θ as 25° and 50° to show the most typical cases in practical engineering.

$$b_w = \frac{0.95h_w cos\theta}{\sqrt{\lambda h}} \qquad (4.6)$$

Decanini and Fantin (1986) used a number of tests on masonry frames under the lateral loading. They offered two sets of equations for various masonry states. The change in the strut width versus parameter $h\lambda$ is illustrated in Figure 4.5.
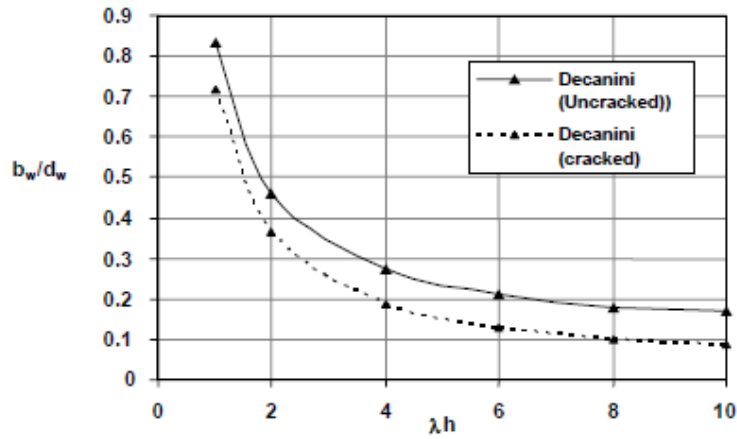
Figure 4.5 Variation of the Ratio b_w/d_w as a Function of the Parameter h.λ
(Decanini & Fantin, 1986)

Lastly, in 1992, a constant value was given for the valuation of b_w by Paulay and Priestley. These findings have been considerably beneficial for the design purposes.

$$b_w = d_w/4 \qquad (4.7)$$

Figure 4.6 illustrates and compares all the expressions mentioned earlier in this chapter.
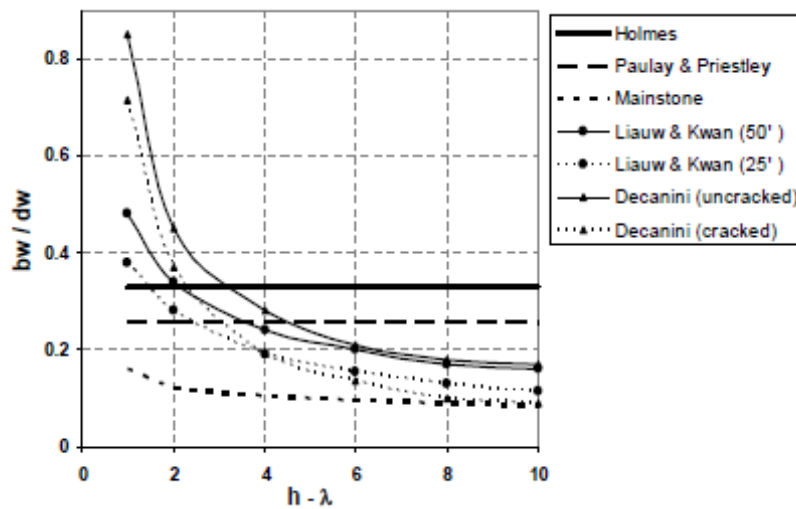
Figure 4.6 Variation of the Ratio b_w/d_w as a Function of the Parameter h.λ (Zhang, 2006)

26

4.2 Cyclic Behavior of the Infill Masonry

The masonry strut hysteresis model is adopted by equivalent struts. This model has five rules which consider the possibility of various stress paths (Figure 4.7). On the other hand, the shear strut adopts a bilinear hysteresis rule (Figure 4.8) (Zhang, 2006).

Figure 4.7 Hysteretic Model for Axial Cyclic Behavior (Crisafulli, 1997)
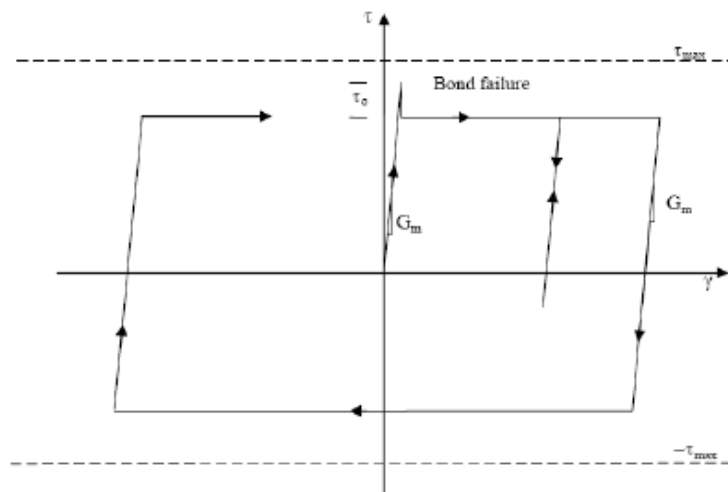
Figure 4.8 Bilinear Hysteretic Model for Shear Cyclic Behavior (Crisafulli, 1997)

The next chapter is focused on using pushover analysis of this model. The cyclic model for the infill wall is not a debatable subject. The original study by Crisafulli (1997) may provide more details into this subject.

27

Chapter 5

DOUBLE STRUT MODEL STUDIES

5.1 General Information

In this chapter, a reinforced concrete model was created in order to determine the effects of infill wall structures on the building performance. The details of the building model were summarized in Table 5.1. The building is a business centre and there are 4 separate offices on each floor. It has total 6 stories and the building height is totally 18 m. A three dimensional floor view of the building has been created with different design software (Figure 5.1). Exterior and interior walls are designed to be 10 cm wide. The exterior walls have 25% window opening and some interior walls have 27% door opening.

Table 5.1 Details of the building

Details of Structure	
Function of the building	Business Centre
Number of storey	6
Type of concrete	C30
Type of reinforcement	S500
Building height (m)	18
Short direction length (m)	16
Long direction length (m)	20
Floor area (m^2)	320
Floor height (m)	3
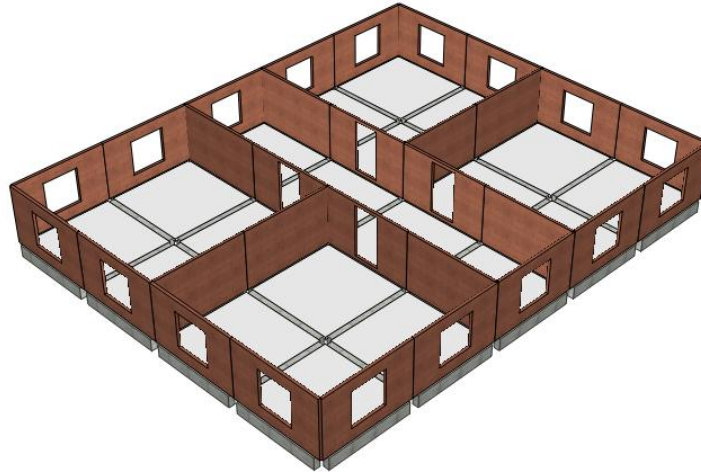
Figure 5.1 3D Floor View

This building model was investigated in 3 different types. Each of the different type of building models have been analyzed as bare frame, AAC infill wall and brick infill wall frame.

In order to analyze the results and behavior of different models under horizontal loads, nonlinear static (pushover) analyses have been carried out.

Different types of buildings were modeled in SeismoStruct analyze software with fiber elements simulating beams and columns. In order to carry out pushover analysis to investigate the displacement capacity of dissimilar models, triangular distributed incremental forces were applied along the structural height and same incremental forces were used in all models.

The importance of the inelastic elements distributed in earthquake engineering is increasing both in research and in application. The general stress-strain case of the cross sections on 3D beam-column elements can be obtained by gathering of the uniaxial nonlinear material behavior of each fiber element they have been divided

into. Therefore, the inelastic behavior is taken into consideration along the element and through the depth of the cross section. These elements do not require to be divided into smaller pieces in many cases; so faster analyses could be made by smaller sized models comparing to the analyses based on displacement in case of being used.

In order to provide the balance conditions of each integration cross section of the elements, the amount of fiber in the cross section used should be defined. The ideal amount of fiber used in the cross section should be large enough to model the stress-strain distribution in the cross section. No wonder this sufficiency depends on the shape of the cross section, the material quality used in the cross section and the level of inelasticity of the element. While 100 fiber elements per cross section can be defined roughly, for cross sections which are complex and show a high level of inelasticity, this number can possibly go over 200. As can be observed clearly, arranging this number properly can be possible by sensitivity practices.

The cross section and element behavior is being modeled with fiber elements in SeismoStruct and each fiber element is defined with uniaxial stress-strain relationship. Afterwards, the stress-strain behavior of the cross sections is obtained by bringing all the fibers' nonlinear uniaxial behavior together. An example of a reinforced concrete beam cross section and the fiber elements involved are shown in Figure 5.2. The column and beam cross sections used in the models are provided in Figure 5.3 and Figure 5.4, respectively. Mander et al. (1988) nonlinear concrete model and Menegotto-Pinto (1973) steel model were used in all models. The materials used in the column and beam elements are given in Table 5.2.
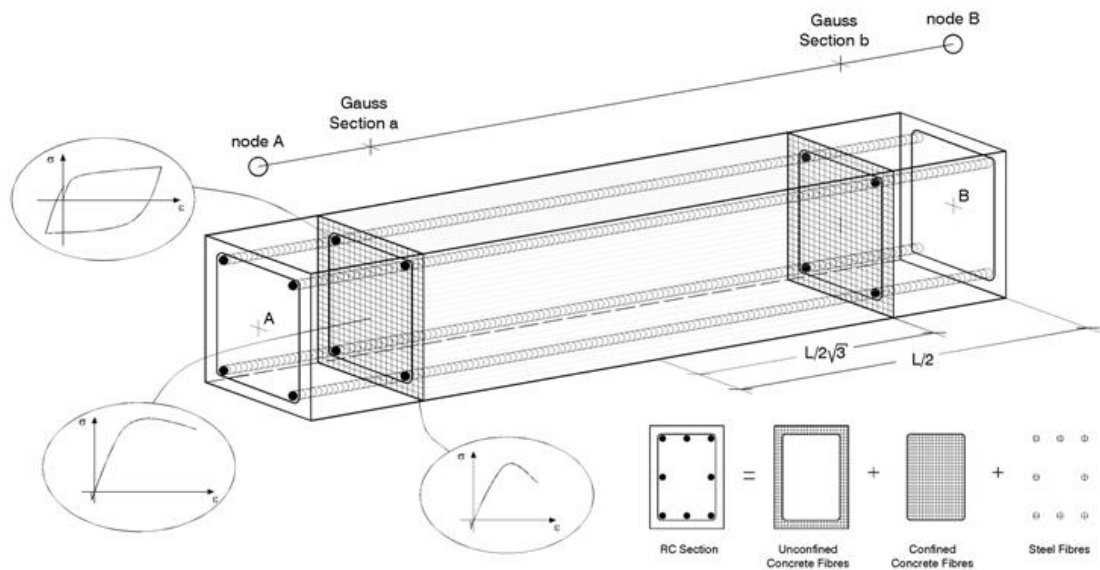
Figure 5.2 Discretization of RC Cross-Section in a Fibre-Based Model (SeismoSoft)
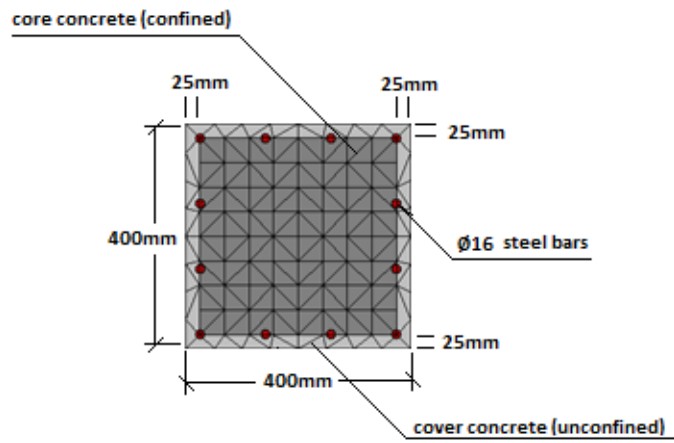
Figure 5.3 Column Sections
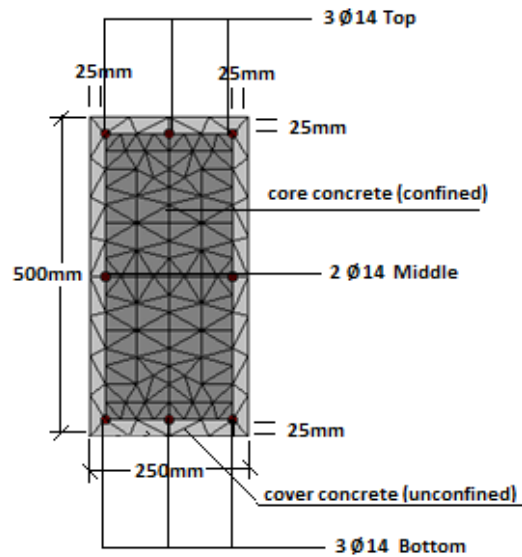
Figure 5.4 Beam Sections

Table 5.2 Details of beams and columns materials

Details of Structure	
Type of concrete	C30
Confinement factor	Confined concrete: 1.2
	Unconfined concrete: 1.0
Type of reinforcement	S500

Within the definition of engineering based on performance, determining the moments when the structural elements reach specific performance limits (eg. structural damage, collapse) are important parameters in the analysis and these are detailed in SeismoStruct. These criteria are examined in 4 different ways in the sample models.

- *Yielding of steel:* it can be identified by checking for (positive) steel strains larger than the ratio between yield strength and modulus of elasticity of the steel material. [Typical value: +0.0025]

- *Spalling of cover concrete:* it can be recognised by checking for (negative) cover concrete strains larger than the ultimate crushing strain of unconfined concrete material. [Typical value: -0.002]

- *Crushing of core concrete:* it can be verified by checking for (negative) core concrete strains larger than the ultimate crushing strain of confined concrete material. [Typical value: -0.006]

- *Fracture of steel:* it can be established by checking for (positive) steel strains larger than the fracture strain. [Typical value: +0.060]

In the pushover analysis a load factor λ is calculated by the program according to the horizontal load values previously defined at each push step (5.1).

$$\lambda_i = \frac{p_i}{p_0}$$

(5.1)

The incremental load value p_i, at any analysis step *(i)* is the multiplication of the nominal value defined previously p_0 and the load factor of that step λ_i.

5.2 Input Parameters in SeismoStruct

According to the aforementioned, the first parts of the analyses were made by SeismoStruct analysis software (SeismoSoft, 2013).

SeismoStrut can be defined as fiber-based finite element package. It is able to anticipate the large displacement behavior of space frames under static or dynamic loading. It is supposed to be contemplated the geometric nonlinearities and material inelasticity of the masonry.

The input parameters to analyze masonry infill panels can be separated into two dissimilar categories. One of these focuses on the mechanical and geometrical parameters and the other focuses on the empirical parameters (Crisafulli, 1997).

5.2.1 Mechanical and Geometrical Parameters

In order to describe the behavior of the masonry struts, several mechanical and geometrical parameters are necessary. The required variables such as input data are given in the form of a list below. Also, suggestions are given in order to select the values. Finally, the values are applied.

a) **Compressive strength $f_{m\theta}$:** this can be defined as the parameter which primarily takes the resistance of the strut under control (Zhang, 2006).

b) **Elastic modulus E_m :** this is a parameter to show the initial slope of the strain-stress curve and its values display a great variation. 7000 MPa for brick and 2728 MPa for AAC infill wall used in the analysis of the models.

c) **Tensile strength f_t :** it is indicates the tensile strength of the masonry or the bond-strength of the interface between frame and infill panel. It existence proposes a general scope within the model. However it can even be acceptable as zero because it is significantly less than the compressive strength with an insignificant influence on the overall response (Varum, 2003).

d) **Strain at max stress ε_m :** it shows the maximum strain level of strength and influences by the modification of the secant stiffness of the ascending branch of the stress-strain curve. It has been found that the value 0.0012 can give sufficient outcomes (Smyrou et al., 2006).

e) Ultimate strain ε_u : it can be used in order to control the decreasing branch of the stress-strain curve. It is modeled by using a parabola in order to get a better control of the strut response. The decrease in the compressive strength is much smoother for the larger values such as 20 ε_m. The amount of 0.024 is suggested by Smyrou et al. (2006).

f) Closing strain ε_{cl} : it describes the strain after the closing of the cracks partially. It allows the compression stresses to develop. The influence is not taken into account in the analysis for larger values. Varied values between 0 and 0.003 are suggested. In the models, the value 0.003 is used (Zhang, 2006).

g) Bond shear strength τ_o and Coefficient of friction μ : with direct shear strength or design specifications the values for parameters can be obtained. A statement in order to reducing the commonly overestimated values from shear tests was presented Mann and Muller (1982). The τ_o values range between 0.1 and 1.5 MPa was indicated and a amount of 0.3 for μ for design purposes were reported by Paulay and Priestley (1992). On the other hand, Atkinson et al. (1985) were found to express a range from 0.70 to 0.85 for μ. In the models, τ_o and μ have been matched with the values 0.3 and 0.7 Mpa (Smyrou et al., 2006).

h) Maximum shear stress τ_{max} : it describes the maximum acceptable shear stress in the infill panel and is possible to be predicted with the statements proposed in the modified Mann and Muller's theory (Crisafulli, 1997), by the normal mode of failure. 1MPa is adopted as a value (Smyrou et al., 2006).

i) Horizontal and Vertical offset, x_{oi} and y_{oi} : these are to show the reduction in the dimensions of infill panel as a result of the depth of the frame members.

j) Vertical separation between struts h_z : contact length values of 1/3 and 1/2 are proposed by Crisafulli (1997). Stafford Smith (1966) defined the contact length z in the Equation (4.1). The same researcher also presented the dimensionless relative stiffness parameter λ (shown in the Equation 4.1 and 4.2).

k) Thickness t_w: this represents the thickness of the panel. As stated previously, inner and outer walls were considered 10 cm wide in all models.

l) Area of strut A_1 : it is the product of panel thickness and the equivalent width of the strut. This usually varies from 10% to 25% of the diagonal infill panel. Several experimental statements for the assessment of the equivalent width exist (Zhang, 2006).

m) Residual Area of the strut A_2 : As a result of the infill panel cracking, the contact length between the frame and the infill decreases when the lateral displacement and consequently the axial displacement increases. As a consequent the axial displacement increases and it affects the area of equivalent strut. With the purpose of gaining generality and taking the control of the stiffness difference and axial strength of the strut, the residual area value is added in the model as a percentage of the initial area. Decanini and Fantin (1986) have proposed the ratio A_2/A_1 and this was used for the calculation of the residual are caused by cracking.

n) Opening: the influence of the openings was studied by decreasing the initially calculated equivalent strut area and stiffness of the infill panels as well (Zhang, 2006). In analyze models the opening ratios which will be calculated is 25% and 27%. It will also be transformed into a reduction of A_1.

5.2.2 Empirical Parameters

A definition is necessary in the model where several experimental parameters participated. Below is the brief description on the definitions:

a) γ_{un} : this explains the unloading modulus in proportion to E_{mo} and changes the internal cycles but not the envelope.

b) α_{re}: this estimates the strain where the loop reaches the envelope after unloading.

c) α_{ch}: this estimates the strain where the reloading curve has an inflexion point which controls the fatness of the loop.

d) β_a: this explains the auxiliary point which is used to explain the plastic deformation after the full unloading.

e) β_{ch} : this explains the stress on the inflection point exhibited by the reloading curve.

f) γ_{plu} : it explains the modulus of the hysteretic curve at zero stress after the full unloading in proportion to E_{mo} .

g) γ_{plr} : this explains the modulus of reloading after the full unloading.

h) e_{x1} : this takes the control of the effect of ε_{un} in the degradation stiffness.

i) e_{x2} : this increases the strain where the envelope curve is reached when the unloading is complete and shows the cumulative damage in the repeated cycles. When the repeated consecutive cycles exist in the same inner loops, it becomes significant.

j) γ_s : this shows the panel stiffness ratio on shear spring.

k) α_s : the ratio of the highest shear stress to the average stress in the panel is shown by the reduction shear factor.

Crisafulli (1997) have obtained the proposed values (Table 5.3) after the calibration of empirical data. On the other hand, for the four of the parameters, the out-of-range values were used. This was after the Smyrou et al. (2006) have carried out the calibration studies.

Table 5.3 Empirical parameters

	Suggested Values	**Limit Values**	**Used Values**
γ_{un}	1.5-2.5	≥ 1	1.7
α_{re}	0.2-0.4	≥ 0	0.2
α_{ch}	0.3-0.6	0.1-0.7	0.7
β_a	1.5-2.0	≥ 1	2.0
β_{ch}	0.6-0.7	0.5-0.9	0.9
γ_{plu}	0.5-0.7	0-1.0	1.0
γ_{plr}	1.1-1.5	≥ 1	1.1
e_{x1}	1.5-2.0	≥ 0	3.0
e_{x2}	1.0-1.5	≥ 0	1.0
γ_s	0.5-0.75		0.7
α_s	1.4-1.65		1.5

5.3 Case Study 1

In this example as can be seen in Figure 5.1 the entire floors including the ground floor is being used as offices. Three dimensional view of the building is given in Figure 5.5. The analysis is carried out as bare frame, AAC infill wall and brick infill wall frame as stated previously. Figure 5.6 provides the capacity curves of the models at the end of the analysis.
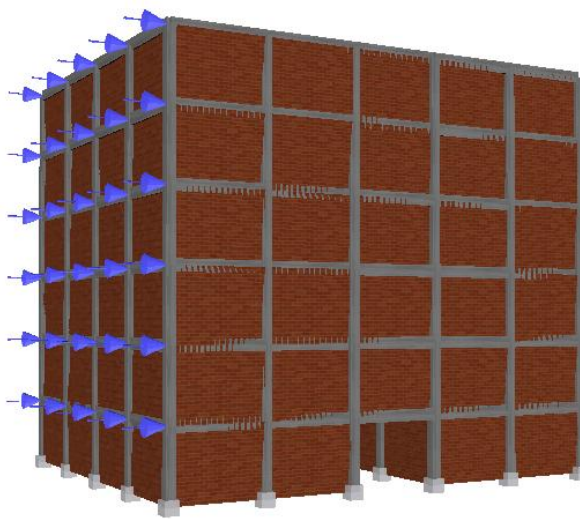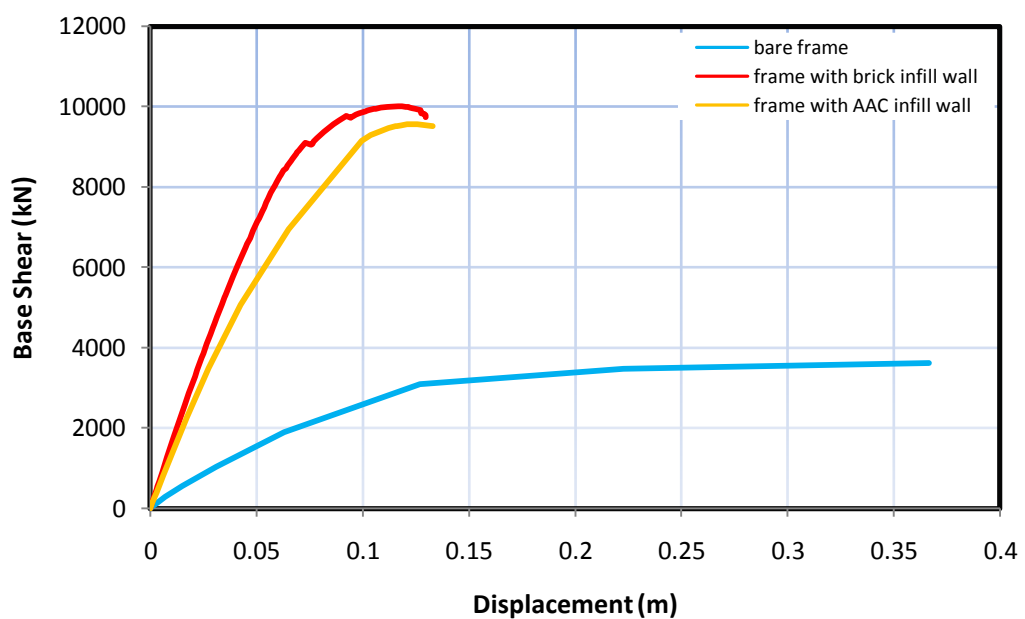

Figure 5.5 3D View of Case Study 1

Figure 5.6 Capacity Curves for Case Study 1 utilizing dissimilar Infill Wall Materials

When the capacity curves are examined it has been observed that the contribution of infill wall models on the building performance is considerably higher than the bare frame model. It has also been observed that the brick wall model receives more base shear force than the other two models.

The building performance has been found out by determining the load factor λ_i at the moment that goes over the border limits of the different type materials (Table 5.4).

Table 5.4 Performance points for case study 1 using different infill wall models

Building Type	Performance Point							
	Yielding of steel		Spalling of cover concrete		Crushing of core concrete		Fracture of steel	
	Beam (λ)	Column (λ)	Beam (λ)	Column (λ)	Beam (λ)	Column (λ)	Beam (λ)	Column (λ)
Bare Frame	8.405	13.747	16.057	15.452	-	-	-	-
Frame with AAC infill wall	30.88	40.702	-	42.35	-	-	-	-
Frame with brick infill wall	35.8	38.718	-	44.257	-	-	-	-

In this table, load factor λ is the value of the damage level. When the elements reaches the damage level, using a different color SismoStruct painting that elements to shows the damaged level. Each damaged level has different paint colors. In this example, the brown colors show that elements exceed the limit of yielding of steel and green colors show that elements exceed the limit of spalling of cover concrete (Figure 5.7).
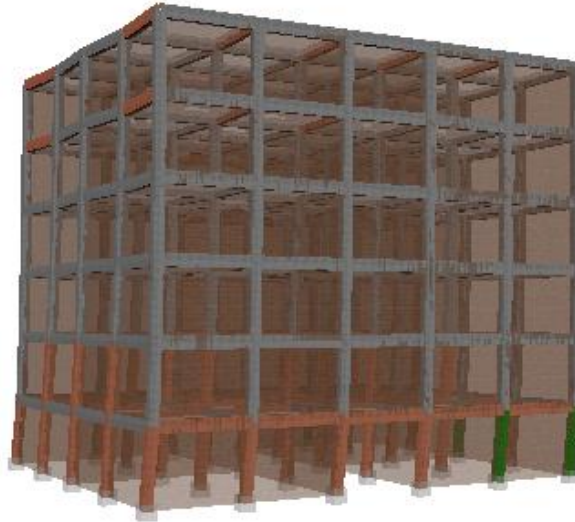
Figure 5.7 Damaged Level of Brick infill Walls of Case Study 1

When the building performance models are analyzed the first border values are gone over at the beams as expected. In the bare frame model the cover concrete on the columns have received damage earlier than the beams. On the other hand the cover concrete on the beams has not reached the damage level at infill wall models. At the beginning, steel has reached the border value earlier on the column elements of the brick infill wall model comparing to the AAC infill wall model. However the cover concrete of the brick wall model has been damaged later than the AAC infill wall model.

The storey drift ratios of the models have been determined as soon as the cover concrete on the columns started to be damaged. The values found out with the averages of each floor's nodal points have been shown in Figure 5.8. According to this, it has been observed that the brick infill wall model has received less displacement than the AAC infill wall model, especially for the top floor level.
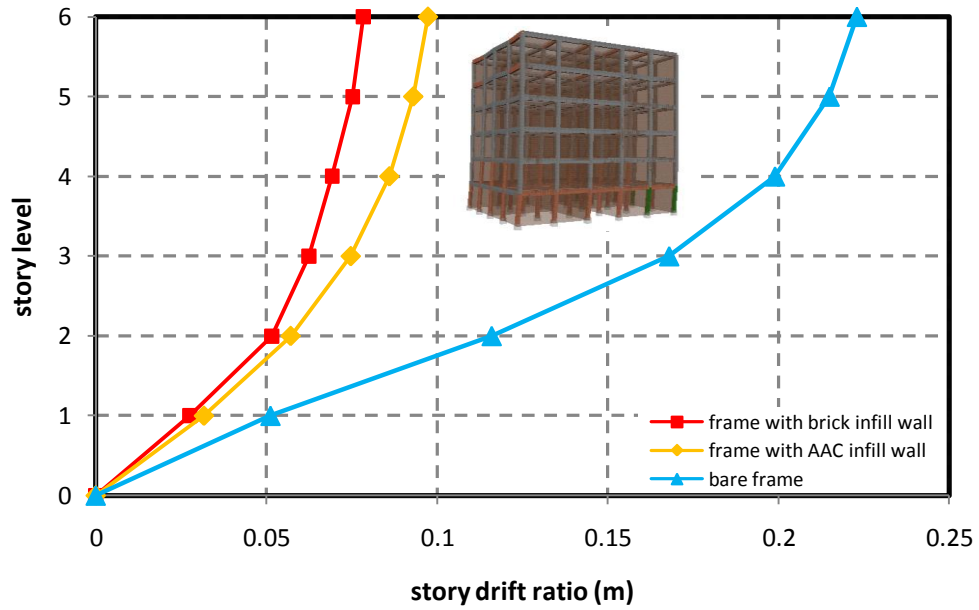
Figure 5.8 Storey Drifts Ratios for Case Study 1

5.4 Case Study 2

Frame system of this example is the same of first example. However, here, the ground floor of the building has been designed as car park and the floor height has not been changed. Three dimensional view of the building has been given in Figure 5.9. At the end of the analyses, the capacity curves of the models have been provided in Figure 5.10.

Figure 5.9 3D View of Case Study 2

Figure 5.10 Capacity Curves for Case Study 2 utilizing dissimilar Infill Wall Materials

When the capacity curves are examined, it can be seen that the performance graph of the both infill wall models are generally similar. However, the brick wall model has received more base shear force and more displacement than the AAC wall model. Building performances are given in Table 5.5 and storey drift values are shown in Figure 5.11.

Table 5.5 Performance points for case study 2 using different infill wall models

Building Type	Performance Point							
	Yielding of steel		Spalling of cover concrete		Crushing of core concrete		Fracture of steel	
	Beam (λ)	Column (λ)	Beam (λ)	Column (λ)	Beam (λ)	Column (λ)	Beam (λ)	Column (λ)
Bare Frame	8.405	13.747	16.057	15.452	-	-	-	-
Frame with AAC infill wall	17.294	12.883	-	18.561	-	-	-	-
Frame with brick infill wall	18.528	12.751	-	19.605	-	21.515	-	-

When the building performance levels are examined, it is observed that the steel on the columns at the beginning of infill wall models have reached the border value

earlier than the bare frame model. However, afterwards, the cover concrete on the infill wall models has been observed to reach the damage level later than the bare frame model. Generally, both infill wall models have shown similar results and the concrete is not damaged on the beam elements. Yet, the core concrete has reached the damage level on the brick wall model.
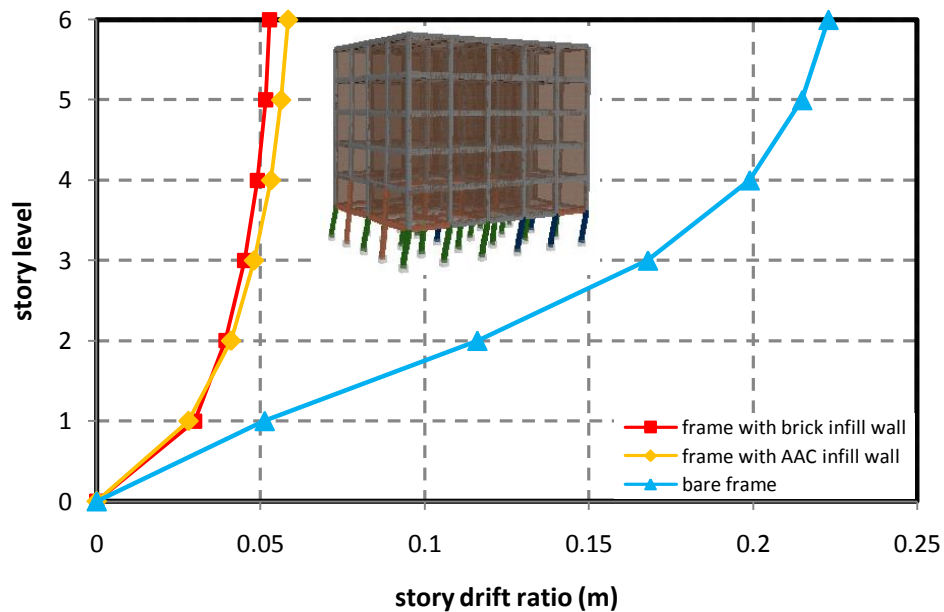
Figure 5.11 Storey Drifts Ratios for Case Study 2

When the Figure 5.11 is examined, it can be seen that the brick infill wall model has more displacement at the first floor than AAC infill wall model; however less displacement was observed on the other floor levels.

5.5 Case Study 3

Frame system of this example is almost same of first example. However, here, the ground floor is designed as 2 separate shops. The structural system of the building was changed comparatively after the first example. Therefore, the bare frame analysis has been carried out again in the example. Three dimensional appearance of

the building has been given in Figure 5.12. As a result of the analyses, the capacity

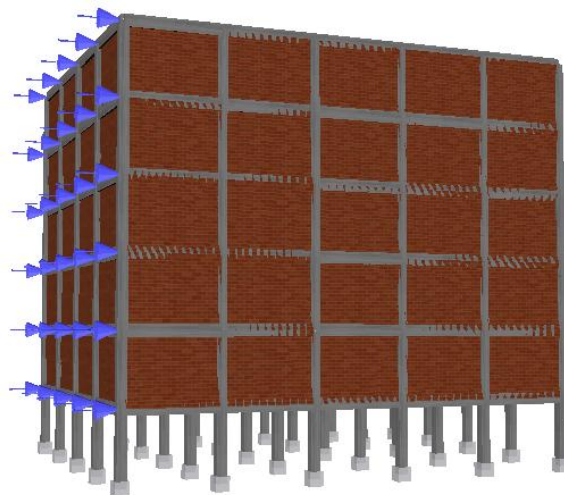curves of the models have been given in Figure 5.13.
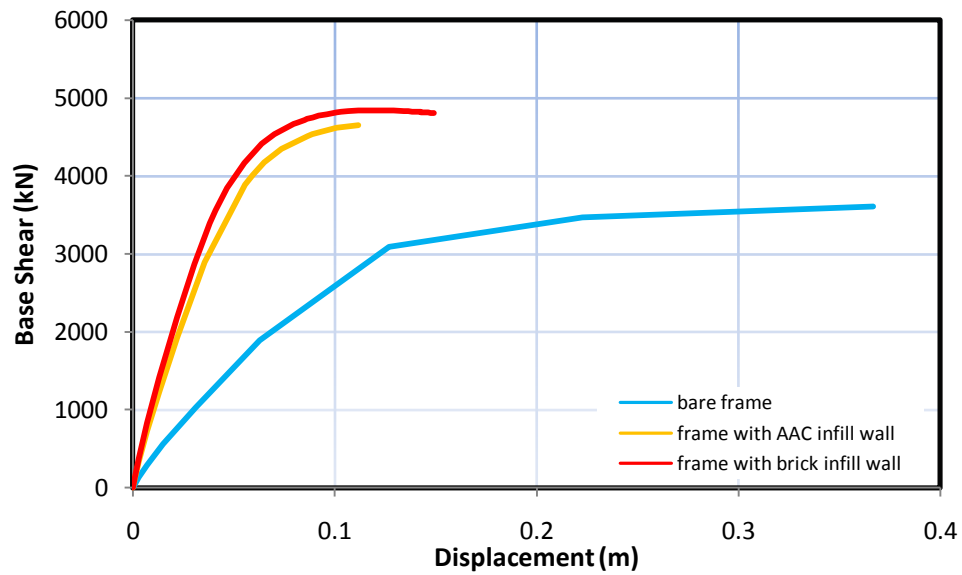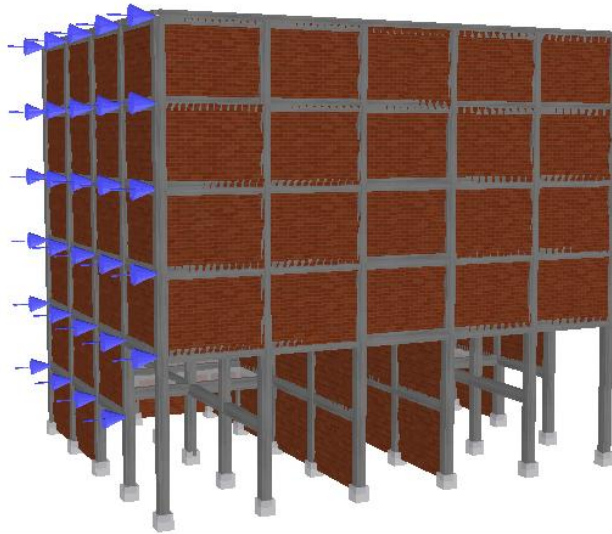

Figure 5.12 3D View of Case Study 3
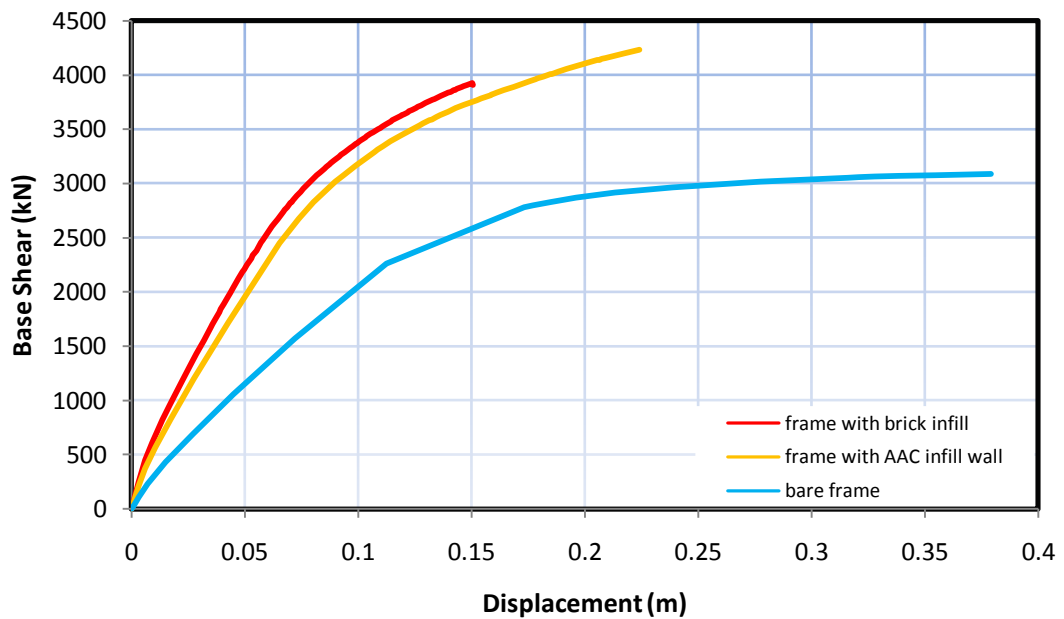
Figure 5.13 Capacity Curves for Case Study 3 utilizing dissimilar Infill Wall
Materials

When the capacity curves are examined, it has been observed that the brick wall

model has received more base shear force and less displacement comparing to the

45

AAC wall model. Building performances are shown in Table 5.6 and storey drift values are given in Figure 5.14.

Table 5.6 Performance points for case study 3 using different infill wall models

Building Type	Performance Point							
	Yielding of steel		Spalling of cover concrete		Crushing of core concrete		Fracture of steel	
	Beam (λ)	Column (λ)	Beam (λ)	Column (λ)	Beam (λ)	Column (λ)	Beam (λ)	Column (λ)
Bare Frame	7.141	10.264	13.711	12.641	-	13.978	-	-
Frame with AAC infill wall	11.143	11.143	18.211	16.063	-	-	-	-
Frame with brick infill wall	11.271	9.928	-	15.552	-	-	-	-

When the building performance levels are examined, the steel reached the border values first on the beams of the bare frame model, the columns of the brick infill wall model and the beams and columns of the AAC infill wall model at the same time. The core concrete has reached the damage level on the bare frame model. The cover concrete has reached the damage level first in the columns for the bare frame and AAC infill wall models. Cover concrete on the beams of the brick infill wall model has not been damaged.
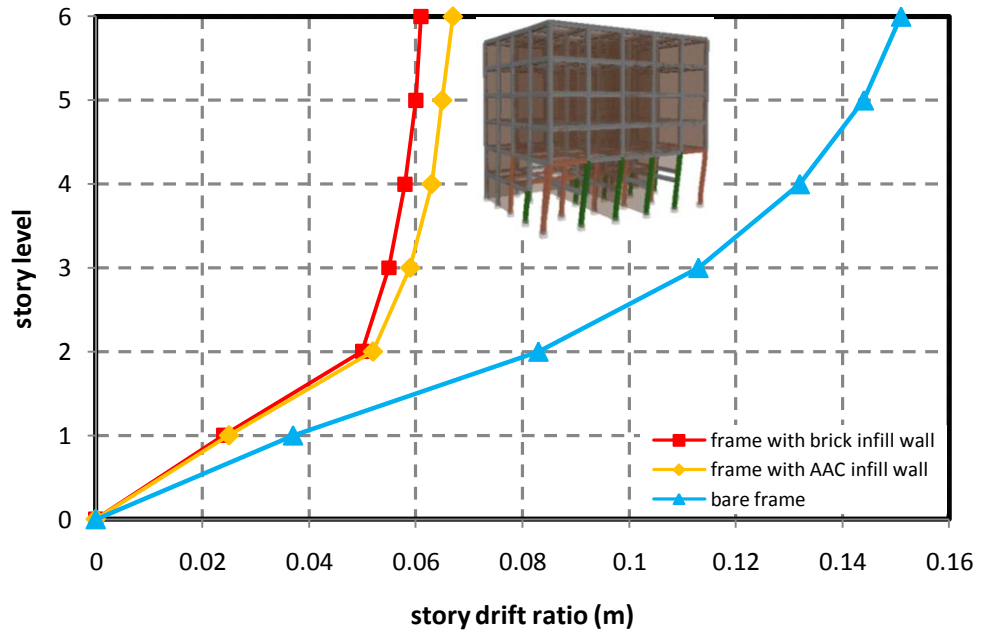
Figure 5.14 Storey Drifts Ratios for Case Study 3

When the Figure 5.14 is examined, it can be seen that the first floors of the brick and AAC infill wall models have the almost same displacement levels however, the other floor levels have more displacement on the AAC infill wall model.

Chapter 6

SINGLE STRUT MODEL

6.1 Model Proposed by P.G. Asteris

Mainstone (1971) and Mainstone and Weeks (1970) have defined equivalent diagonal compression strut with width *w* and thickness *t* in the relationship with 6.1 in order to represent the failure behavior of brick infill wall frames. The modulus of elasticity of this equivalent compression strut has been identified to be the same as the modulus of elasticity of the wall.

$$w = 0.175.(\lambda h)^{-0.4}.d \qquad (6.1)$$

$$\lambda h = h \sqrt[4]{\frac{E_m.t.\sin(2\theta)}{4.E_f.I_c.h}} \qquad (6.2)$$

In which λ is stiffness reduction factor; E_m , *t*, and *h* is elastic modulus, thickness, and height of the brick masonry infill respectively; E_f and *I* is Young's modulus and moment of inertia of the surrounding frame member; *d* is diagonal length of infill panel and θ is angle between the infill diagonal and the horizontal.
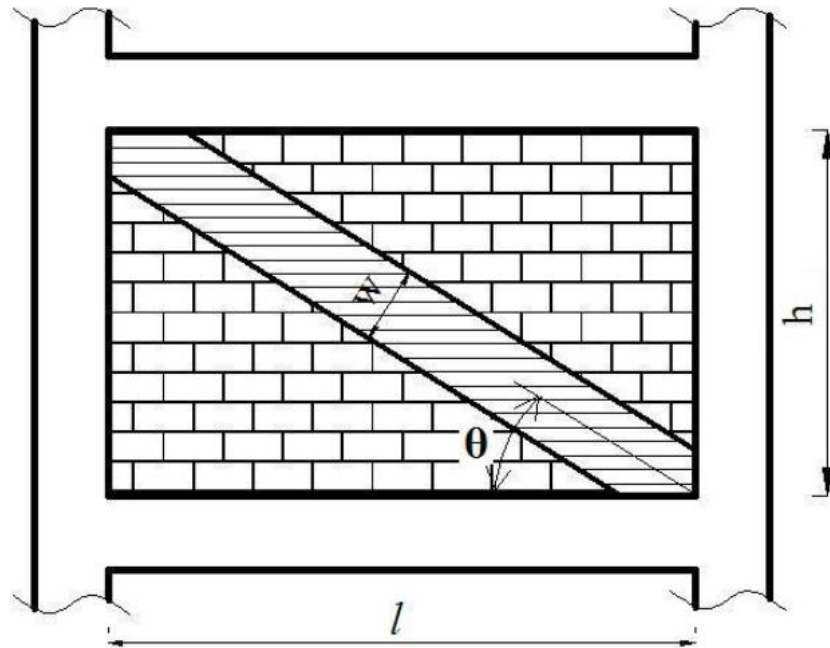
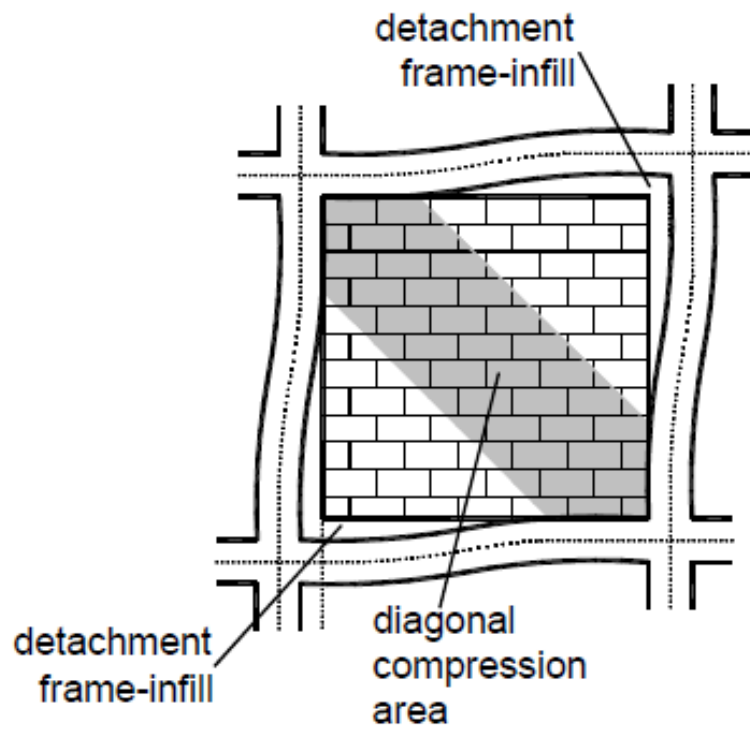Figure 6.1 Equivalent Compression Strut Model (Mainstone, 1971)

Figure 6.2 Sample of Infill frame Under Lateral Loading

Asteris (2003) have suggested 6.3 relationship in order to find out the efficient width of the equivalent compression strut based on the relationship of infill wall suggested by Mainstone (1971).

$$W = 0.175. \lambda_{grap\,h} .(\lambda h)^{-0.4} .d \qquad (6.3)$$

In his studies he has investigated the reduction in the lateral rigidity of the infill wall frames with hollows such as window or door openings by using the method of finite elements. According to this study:

- The lateral rigidity of the infill frames decreases when the proportion of hollows increases. This decrease can reach up to 87% for a frame without a wall (100% for hollow). The rigidity factor λ, is experimentally constant for up to 50% opening.

- The general movements between the frame and the infill are influenced negatively when the location of the opening on the wall gets closer to the compression diagonal.

- Infill walls contribute significantly on the lateral strength of the frame on multi storey buildings. Especially in the cases of three storey frames with infill walls up to 7% reduction has been observed on the lateral displacements.

- The existence of infill walls usually results in a decrease in shear forces on columns. However, the shear forces on the columns with soft story infill wall frames are considerably greater than the values obtained as a result of simple frame analysis.

Asteris (2003) have investigated the cases below in order to understand the effects of the opening on the wall, on the behavior and lateral rigidity of infill frames (Figure 6.3):

a) The cases with or without opening on infill walls

b) The proportion of the opening (opening area/wall area): proportions as 4.00%, 9.00%, 16.00% and 25.00%;

c) With this proportions the location on the wall according to the compression diagonal space has been investigated as three different cases:

- Case A: at the bottom of the opening compression diagonal

- Case B: on the opening compression diagonal

- Case C: on the top of the opening compression diagonal

opening percentage %	opening position		
	A outside and down left of the diagonal	B upon the diagonal	C outside and up right of the diagonal
0.00			
4.00			
9.00			
16.00			
25.00			
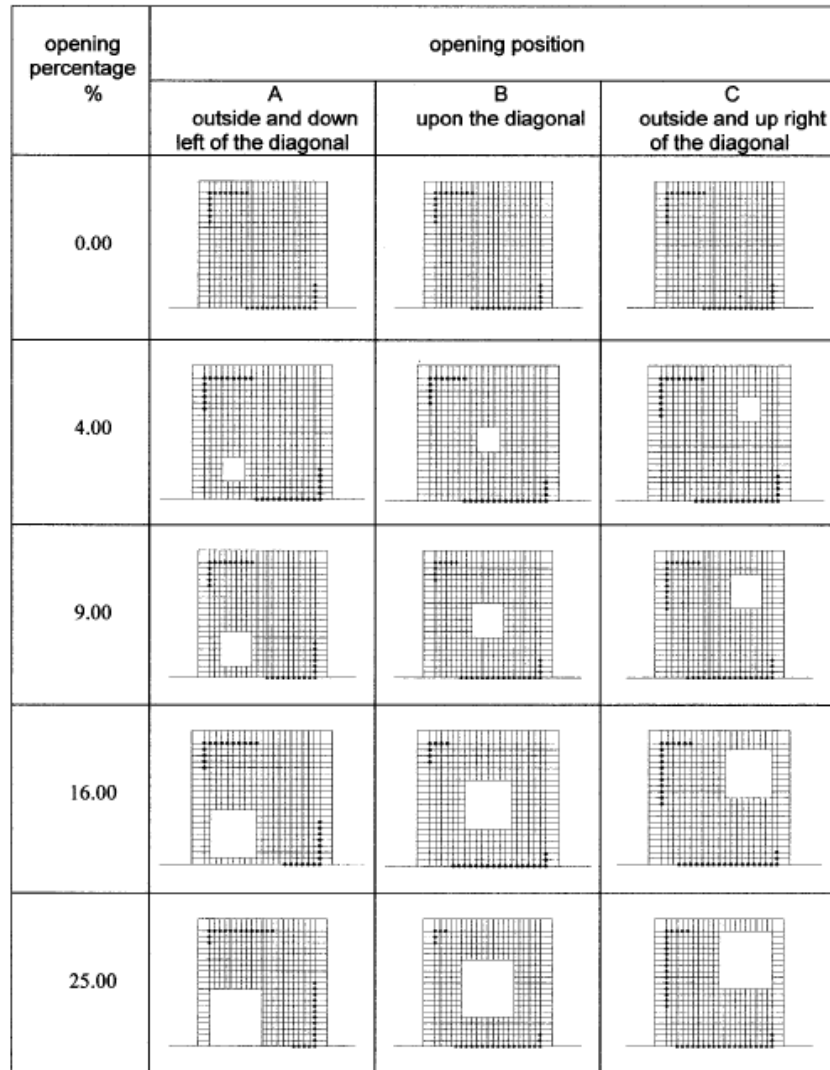
Figure 6.3 Contact/Interaction Areas between Infill Masonry Wall and Surrounding Frame for Different Opening Percentages (Asteris, 2003)

Figure 6.4 shows the change in λ factor as the function of opening proportion for the case B. On the other hand, Figure 6.5 presents the values of λ factors obtained for the 3 different opening cases which were investigated by Asteris P.G. (2003). The higher values of the rigidity factor occur in cases when it is over the opening compression diagonal.

Figure 6.4 Stiffness Reduction Factor λ of Infilled Frame in Relation to Opening Percentage (Asteris, 2003)

Figure 6.5 Stiffness Reduction Factor λ of Infilled Frame in Relation to Opening Percentage for Different Positions of Opening (Asteris, 2003)

The rigidity reduction factor obtained in Figure 6.4 and Figure 6.5 can be used to identify the efficient width of the diagonal compression strut closer to the ideal.
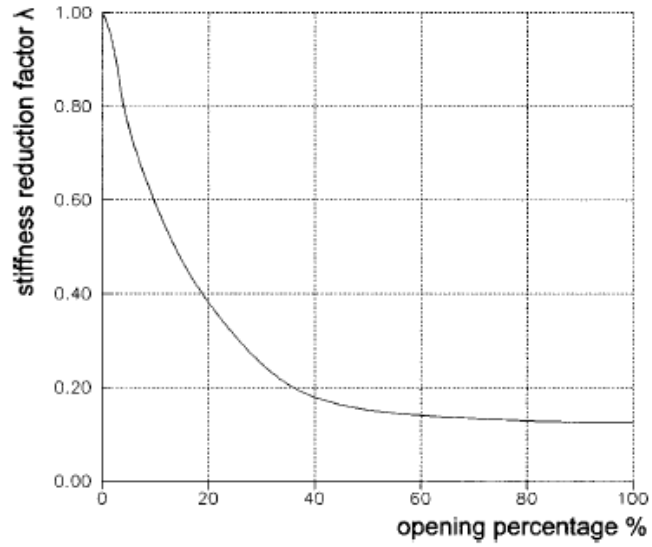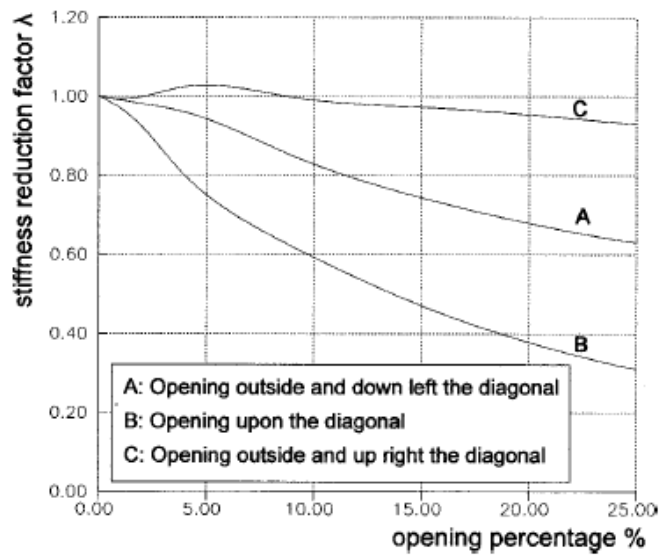
Chapter 7

SINGLE STRUT MODEL STUDIES

7.1 General Information

In this section, 3 different building models have been created and the behaviors of these structures under horizontal loads have been investigated in order to identify the effects of infill wall structures on the building performance. All of the models created with existing buildings have different characteristics, bearing systems with different sizes and different heights.

Each model created was analyzed in 3 different ways as a bare frame, brick infill wall and AAC infill wall and the results have been compared. The mechanic models of the reinforced concrete bearing systems have been created identical to the real ones and then cross struts against each infill wall have been added to these mechanic models. All of the characteristics of the compression struts representing the infill walls have been identified according to the criteria proposed by Asteris (2003). All struts modeled only to work under compression.

For the creation of the three dimensional models of the structures and their structural analysis, Probina Orion 2013 software has been used. The shell elements used in this software is based on the formulations suggested by Wilson (2002).

All of the models have been designed with brick and AAC infill walls of 20 cm exterior walls and 10 cm interior walls. For the calculations of the wall weight brick

walls has been considered as 13 kN/m^{3}design load and 7.0 kN/m^3 for AAC wall. Interior and exterior plaster of brick walls has been taken as 6 mm as used in the experiments and the design load of the plaster used has been taken as 21 kN/m^3. The building weights of each model were calculated using these values.

In order to analyze the results and behavior of different models under horizontal loads, nonlinear static (pushover) analyses have been carried out. Static pushover analysis is nonlinear procedure in which the structural loading compatible with the specified modal shape is incrementally increased. At each increment, the weak hinges and failure modes of structure are found. The performance of the buildings under a specified earthquake force level defined by design spectrum and performance point concept is introduced

The pushover analysis of different models has been carried out by using Sap2000 v15.0 analysis program software. All these different models the nonlinear properties for columns are assumed to be a plastic P-M-M hinge and beams are assumed to be one component plastic moment hinge. The plastic hinges have been identified with the given distributions of reinforcement for each model according to FEMA 356. The plastic hinges of infill walls (P for normal forces) have been assigned on the middle points of the struts.

7.2 Case Study 1

All of the characteristics of the building have been given in Table 7.1. The cross sections of the vertical bearing structural elements are constant throughout the height. The sizes of the columns and beams and thickness of the slab have been summarized in Table 7.2. Existing reinforcement of building in the concrete

members provided in Table 7.3. Figure 7.1 shows the floor plan of the structure and Figure 7.2 shows the openings and infill walls affecting the floor beams. Figure 7.3 and Figure 7.4 shows the brick wall model and AAC wall model in three dimensions, respectively. The building weights of these different models have been given in Table 7.4.

Table 7.1 Details of the building

Details of Structure	
Date of construction	1997
Function of the building	Apartment
Number of storey	4
Type of concrete	C16
Type of reinforcement	S220
Building height (m)	12.875
Short direction length (m)	16
Long direction length (m)	16.80
Floor area (m^2)	268.8
Floor height (m)	2.95
Dynamic and Geotechnical parameters	
Seismic zone coefficient (Ao)	0.3
Allowable bearing pressure (kN/m²)	200.0
Ductility level	High
Horizontal force factor (R)	1.0
Building importance coefficient (I)	1.0
Live load reduction factor (n)	0.3
Spectrum characteristic period (Ta/Tb)	0.15/0.6
Building knowledge level	Medium
Corrosion ratio in the structural elements	0.0
Thermal expansion difference (°C)	0.0
Seismic Code	TDY2007

Table 7.2 Member dimensions of the building

Columns (mm)	400x250, 500x250, 550x250, 600x250, 700x250
Beams (mm)	250x500
Slab thickness (mm)	120

Table 7.3 Existing reinforcement in members of the building

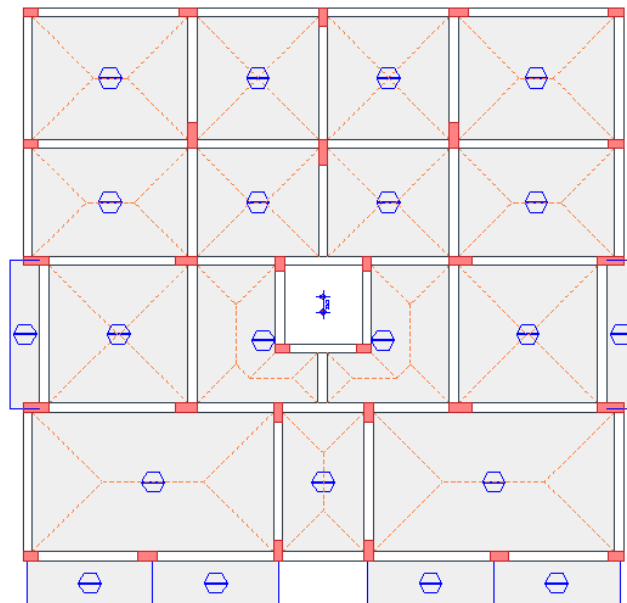| Columns	Longitudinal Rebars: max. %1.5-min. %0.82 Confinements: Ø8/20/10
Beams	Top Reinforcement: %0.5 Bottom Reinforcement: %0.4 Confinements: Ø8/20

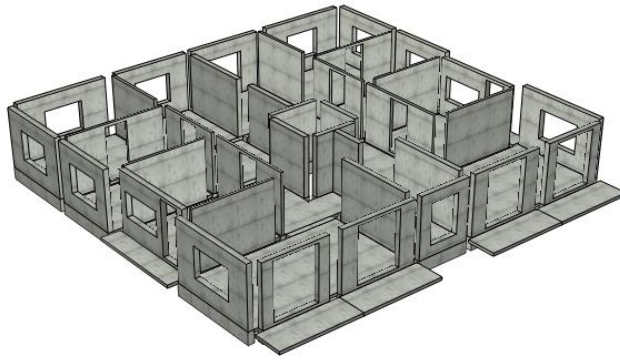Figure 7.1 Floor Plan of the Building

Figure 7.2 3D Locations of Infill Walls on the Beams
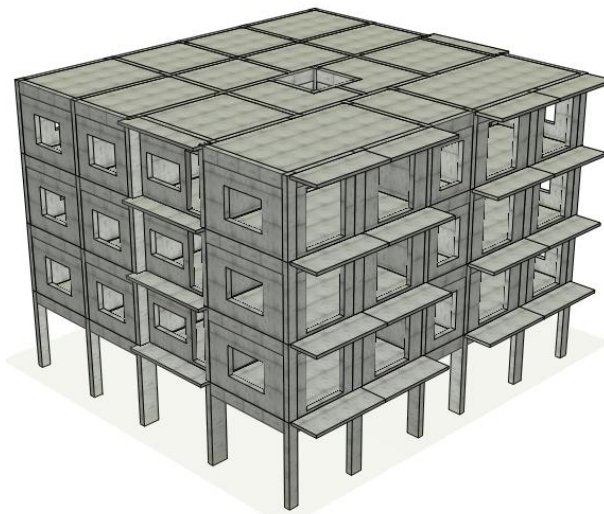

Figure 7.3 3D View of Frame with Brick Infill Wall
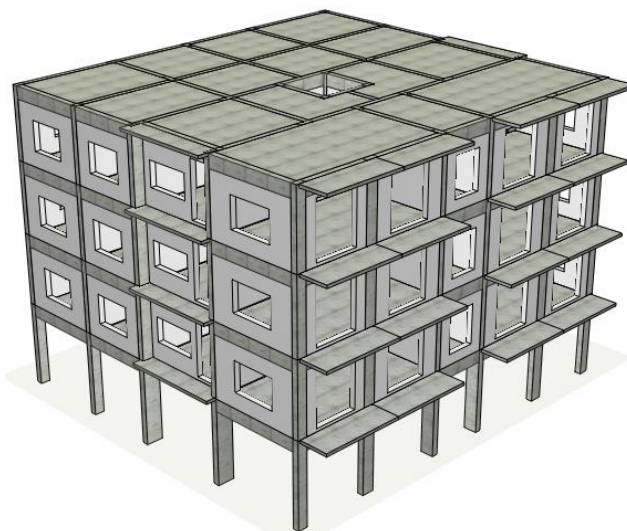
Figure 7.4 3D View of Frame with AAC Infill Wall

Table 7.4 Building weights of different models

Building Type	W(kN)
Bare frame	8802.07
Frame with AAC infill wall	10184.34
Frame with brick infill wall	10853.59

Pushover analysis of different models created for the existing structures have been carried out and the capacity curves have been given in Figure 7.5. Table 7.5 shows the base shear-displacement values of the performance point obtained by the method of ATC 40. The mechanism statuses of the performance points for each model have been given in Figure 7.6, Figure 7.7 and Figure 7.8.
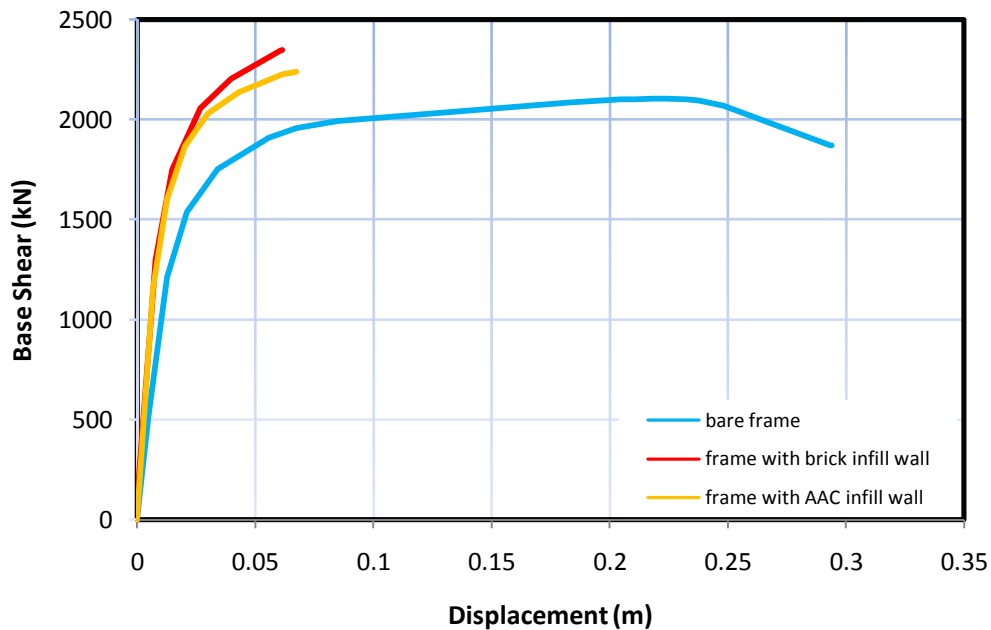
Figure 7.5 Capacity Curves for Case Study 1 utilizing dissimilar Infill Walls Materials

Table 7.5 Performance points for case study 1 using different infill walls material

Building Type	Performance Point		Seismic Performance Level
	Base Shear (kN)	Displacement (m)	
Bare Frame	1746.364	0.034	B-IO
Frame with AAC infill wall	1880.73	0.021	IO-LS
Frame with brick infill wall	1931.406	0.022	IO-LS

Figure 7.6 Bare Frame Mechanism at the Performance Point

Figure 7.7 Frame with AAC Infill Wall Mechanism at the Performance Point

Figure 7.8 Frame with Brick Infill Wall Mechanism at the Performance Point

When the solutions and the capacity curves of the models are compared, the contribution of the infill walls on the behavior can easily be investig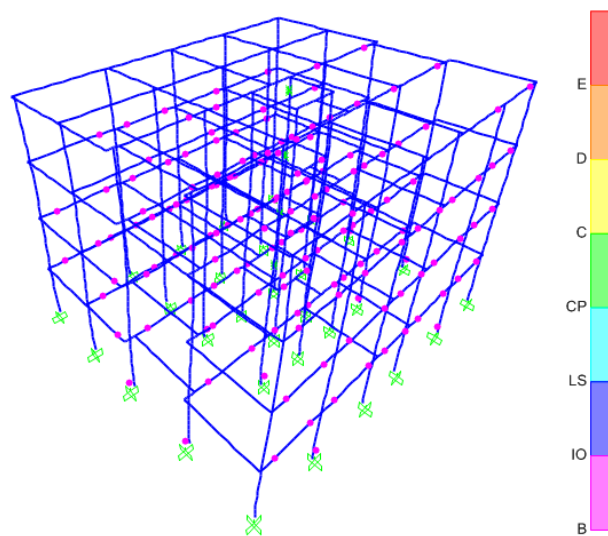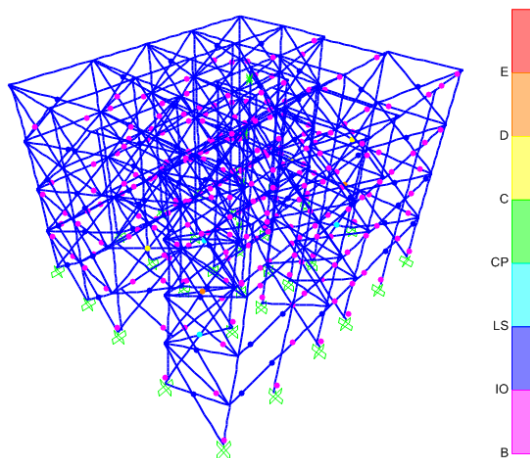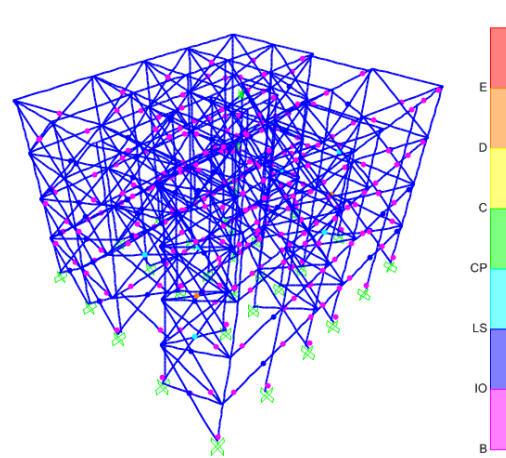ated. If the analysis results of the infill wall models are investigated it has been observed that the first plastic hinges are occurred on the infill walls. It has been stated that the base shear force is increased at the moment that the first plastic hinges occurred. After this stage the plastic hinges occurred on the beams.

It has been observed that the brick infill wall model receives more base shear force compared to the AAC infill wall model and it has approximately the same displacement level with the AAC infill wall model.

The fact that there are large window openings on the front wall of the structure and that the partition walls on the front of the building are used less than the back of the building have created a torsion effect of the building. Therefore, when the damages on the performance points of the infill wall models are investigated it has been observed that a damage level of the structural members specifically on the front has been increased. These damage levels are more for the AAC infill wall model. The geometry of the building is almost a square. This prevents more torsion effect during an earthquake. Therefore, geometry of the building is also an important factor for torsion effect. As seen in the performance point table, performance levels of infill wall models are between IO-LS. However, performance level of bare frame model is between B-IO.

At the end of the analysis the periods of different models has been found. The results obtained shows that the infill walls are significantly effective on the periods of the structure (Table 7.6).

Table 7.6 Periods of different models

Building Type	T(sec)
Bare frame	0.630
Frame with AAC infill wall	0.420
Frame with brick infill wall	0.354

7.3 Case Study 2

Summary of the building are given in Table 7.7. There are two separate shops on the ground floor of the building. The cross sections of the vertical bearing structural elements are changing throughout the height. The sizes of the columns and beams with slab thickness of the structure are given briefly in Table 7.8. The existing reinforcements in the concrete members are provided in Table 7.9. Figure 7.9 shows the floor plans of the structure and Figure 7.10 shows the partition walls and openings that affects the beams on different floor types. Figure 7.11 and Figure 7.12 shows the three dimensional models of brick wall model and AAC wall model, respectively. The building weights of these different models are given in Table 7.10.

Table 7.7 Details of the building

Details of Structure	
Date of construction	2005
Function of the building	Apartment
Number of storey	9
Type of concrete	C16
Type of reinforcement	S220
Building height (m)	25.35
Short direction length (m)	15.20
Long direction length (m)	17.80
Floor area (m^2)	1st Floor: 270.56
	2nd Floor: 58.3
	Normal Floor: 270.56
	Top Floor: 70.6
Floor height (m)	1st Floor: 2.8
	2nd Floor: 2.5
	Normal Floor: 2.8
	8th Floor: 2.8
Dynamic and Geotechnical parameters	
Seismic zone coefficient (Ao)	0.3
Allowable bearing pressure (kN/m²)	300.0
Ductility level	High
Horizontal force factor (R)	1.0
Building importance coefficient (I)	1.0
Live load reduction factor (n)	0.3
Spectrum characteristic period (Ta/Tb)	0.15/0.4
Building knowledge level	Medium
Corrosion ratio in the structural elements	0.0
Thermal expansion difference (°C)	0.0
Seismic Code	TDY2007

Table 7.8 Member dimensions of the building

Columns (mm)	550x300, 700x250, 750x250, 750x300, 700x400, 800x250, 900x30, 1000x250, 1050x300, 1100x250
Shear Walls (mm)	2200x250, 1850x250
Beams (mm)	200x500, 200x550, 200x600
Slab thickness (mm)	120

Table 7.9 Existing reinforcement in members of the building

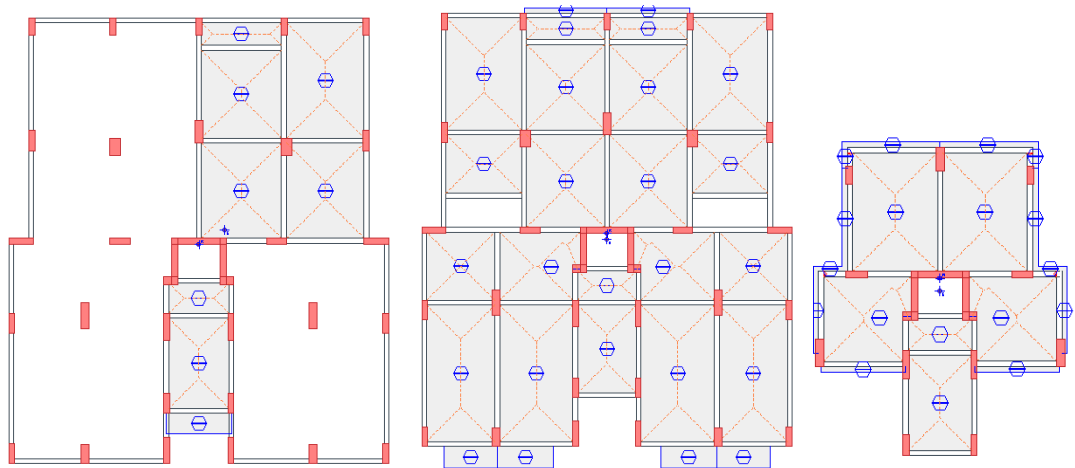| Columns	Longitudinal Rebars: max. %1.17-min. %1.06 Confinements: Ø8/20/10
Shear Walls	Longitudinal Rebars: : Ø12/20 Transverse Rebars: Ø12/20
Beams	Top Reinforcement: %0.55 Bottom Reinforcement: %0.42 Confinements: Ø8/20

Figure 7.9 a) 2st Floor, b) Normal Floor, c) Top Floor Plans of the Building
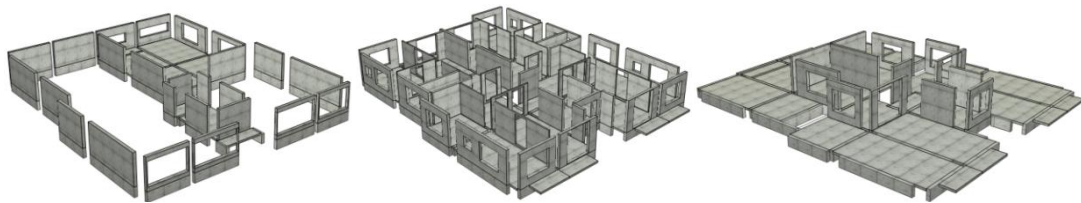

Figure 7.10 3D Locations of Infill Walls on a) 2nd Floor, b) Normal Floor, c) 8th Floor Beams
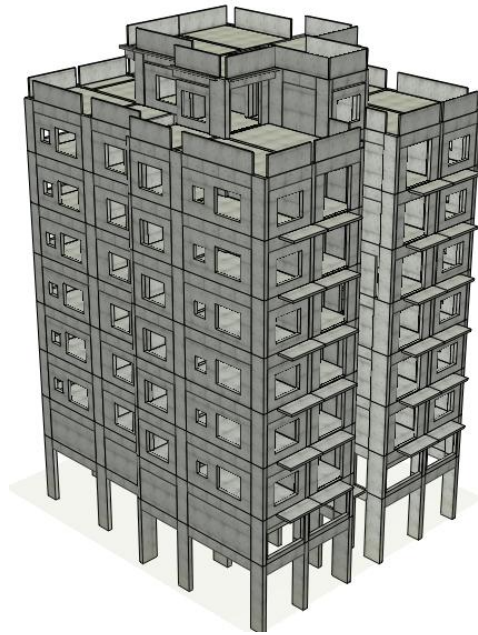
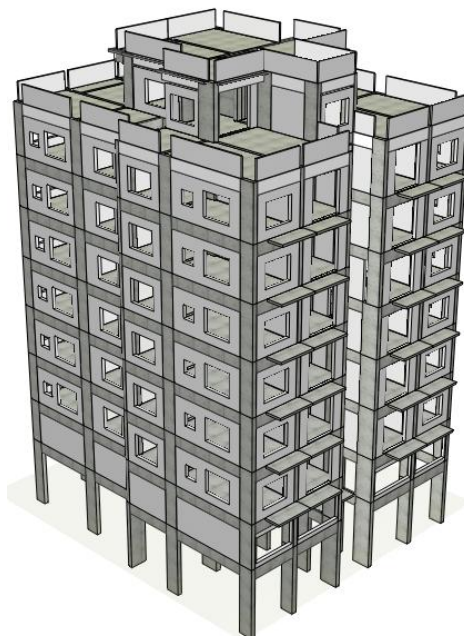Figure 7.11 3D View of Frame with Brick Infill Wall

Figure 7.12 3D View of Frame with AAC Infill Wall

Table 7.10 Building weights of different models

Building Type	W(kN)
Bare frame	19550.62
Frame with AAC infill wall	21456.37
Frame with brick infill wall	23286.53

Reinforced concrete shear walls are widely used in multi storey structural systems in seismically active countries. Since these elements influence the structural analysis results significantly, modeling the shear walls properly is of great importance for the linear and nonlinear analyses of building type structures (Fahjan et al., 2011).

Various analytical models are used in accordance to the Mid-Pier model or shell elements uses for the nonlinear material behavior of the reinforced concrete shear walls. The nonlinear material model of the shell elements can be modeled as a composition of shell element. In this model, reinforcement and concrete in the structural elements are modeled by different texture layers. So the hysteretic behavior of the material can be simulated appropriately (Fahjan et al., 2011).

More realistic results can be obtained by using shell elements in the analysis of building type structures with shear walls. Establishing a network system is required in order to obtain a realistic behavior in shear wall modeling with shell elements. The most important advantage of using shell elements is to enable the interactive complex shear wall systems to be modeled. Even though the shell element equations include drilling degree of freedom, the analytical results show that the results obtained from this drilling degree of freedom are over sensitive and inconsistent

towards the loading conditions and the frequency of network. This case is of great influence on the bending moment of the point where the beams are connected to the shear wall on the same plane with the wall. In order to solve this problem during the engineering applications, the beams connected to the shear wall is modeled by using additional strut elements (rigid beams) generally extended into the shell elements of the shear wall (Figure 7.13) (Fahjan et al., 2011).
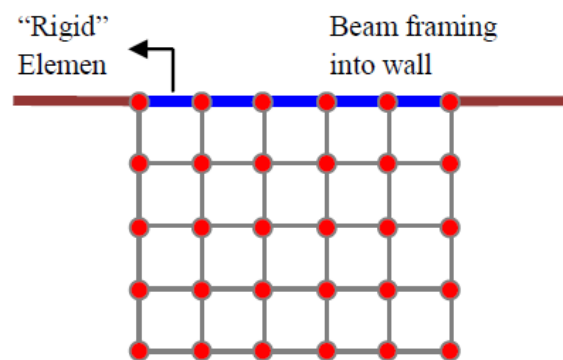
Figure 7-13 Shell Elements Models for Shear Wall (Fahjan et al., 2011)

In this study shear walls were modeled with multi-layer shell elements during the performance analysis. Multi-layer shell elements are based on the principle of composite material mechanic. Shell element is made of several layers of dissimilar thicknesses and these layers are made of materials with different characteristics (Figure 7.14) (Fahjan et al., 2011). Concrete and steel models used in the nonlinear multi-layer material model are shown in Figure 7.15 and Figure 7.16, respectively.
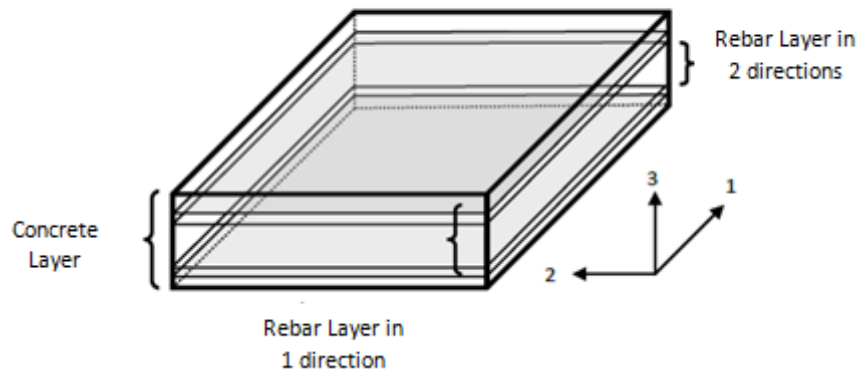
Figure 7.14 Multi-Layer Shell Elements (Fahjan et al., 2011)
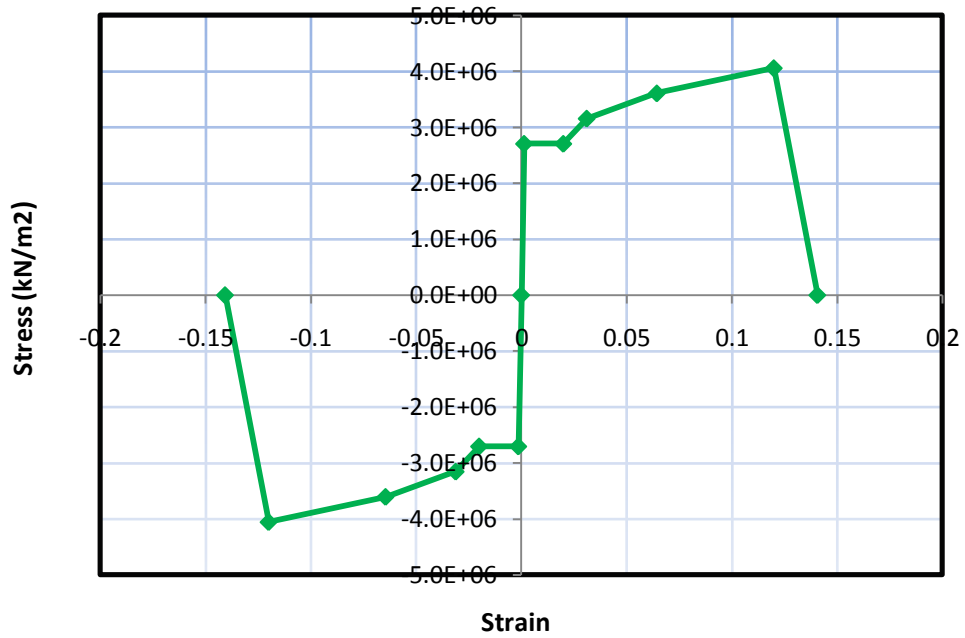
Figure 7.15 Nonlinear Material-Reinforcement Steel Model
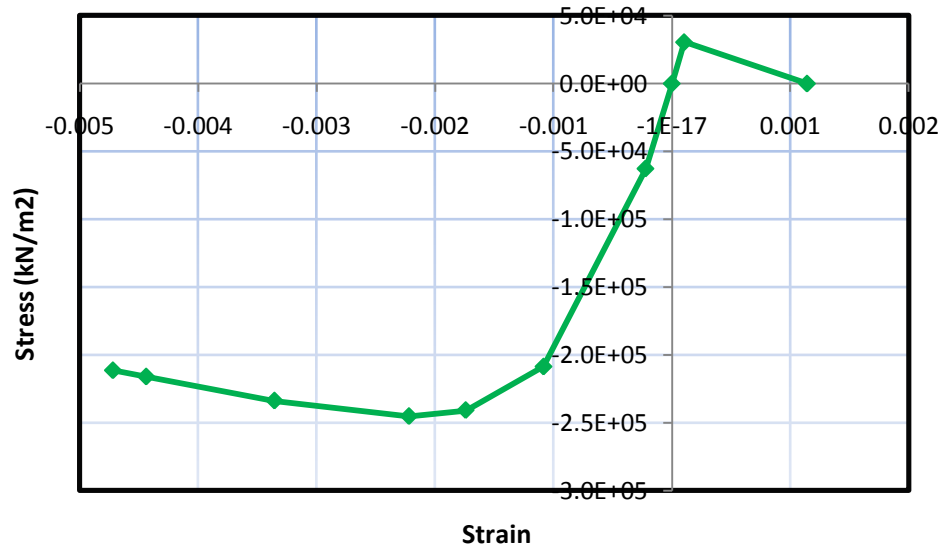
Figure 7.16 Nonlinear Material-Concrete Model

As a result of the performance analysis, the capacity curves of different models are given in Figure 7.17. The base shear force-displacement values of the performance points obtained by ATC 40 method is shown in Table 7.11. The mechanism of the performance points for each model is provided in Figure 7.18, Figure 7.19 and Figure 7.20, respectively. The nonlinear behavior of multi-layer shell can be examined by controlling the stresses in concrete and reinforcement layers (Figure 7.21 and Figure 7.22).
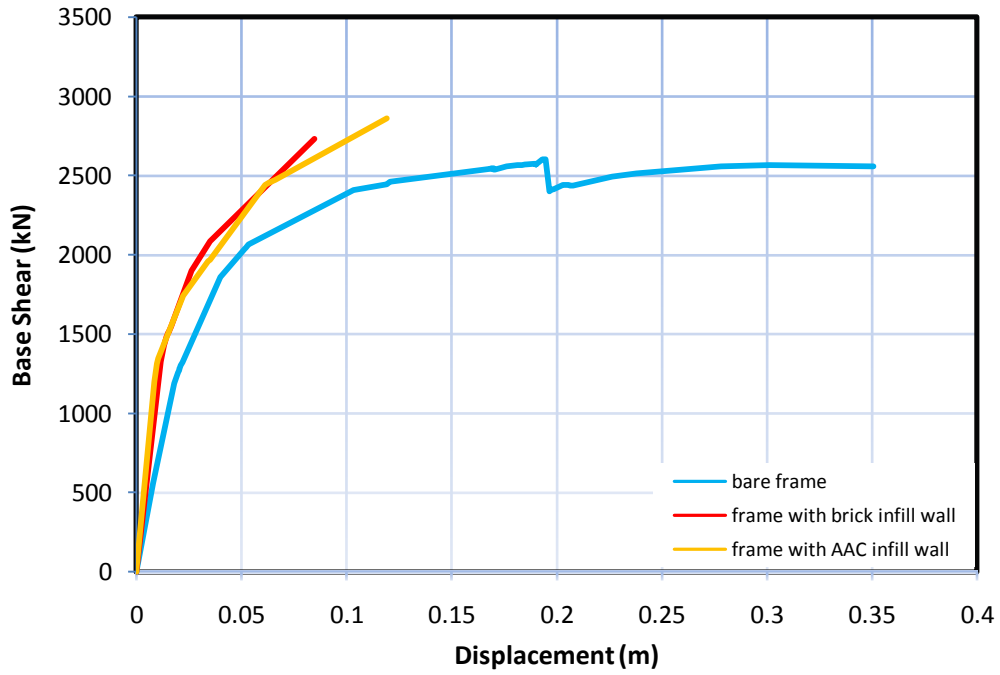
Figure 7.17 Capacity Curves for Case Study 2 utilizing dissimilar Infill Walls Materials

Table 7.11 Performance points for case study 2 using different infill walls material

Building Type	Performance Point		Seismic Performance Level
	Base Shear (kN)	Displacement (m)	
Bare Frame	2075.473	0.055	B-IO
Frame with AAC infill wall	1784.606	0.025	B-IO
Frame with brick infill wall	2023.976	0.032	B-IO
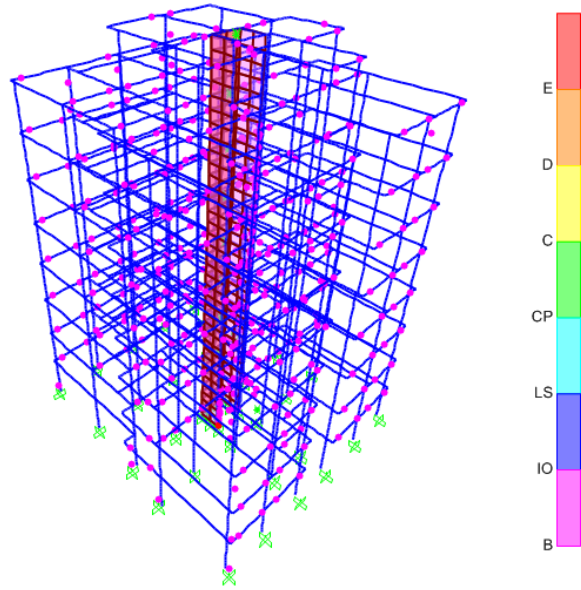
Figure 7.18 Bare Frame Mechanism at the Performance Point
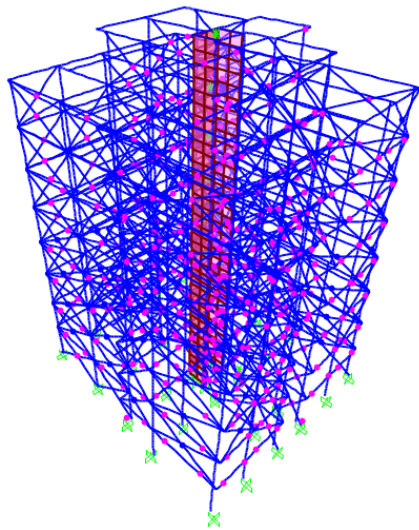
Figure 7.19 Frame with AAC Infill Wall Mechanism at the Performance Point
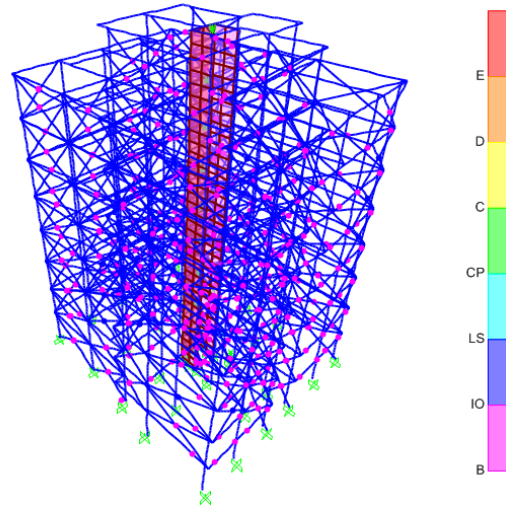
Figure 7.20 Frame with Brick Infill Wall Mechanism at the Performance Point
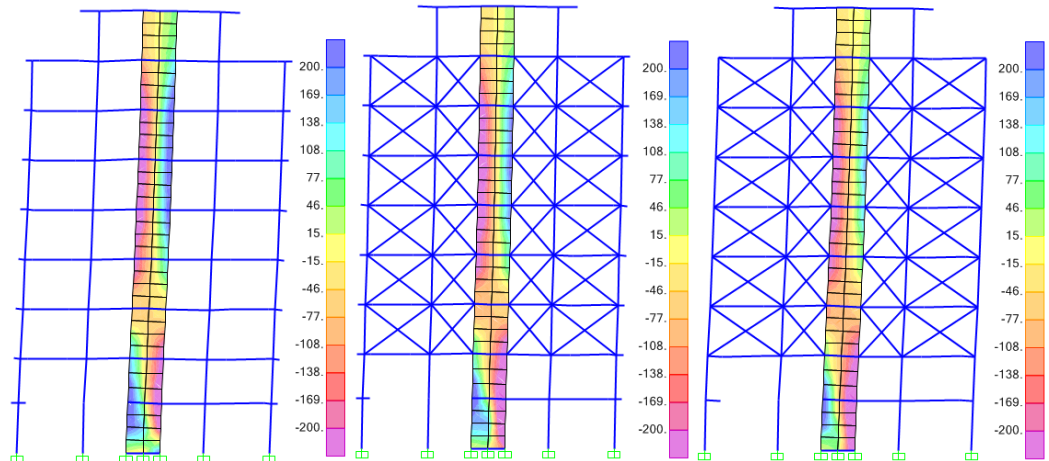
Figure 7.21 Multi Layer Shell Stresses in Concrete Layers at the Performance Points According to a) Bare Frame, b) Frame with AAC Infill Wall, c) Frame with Brick Infill Wall, Respectively
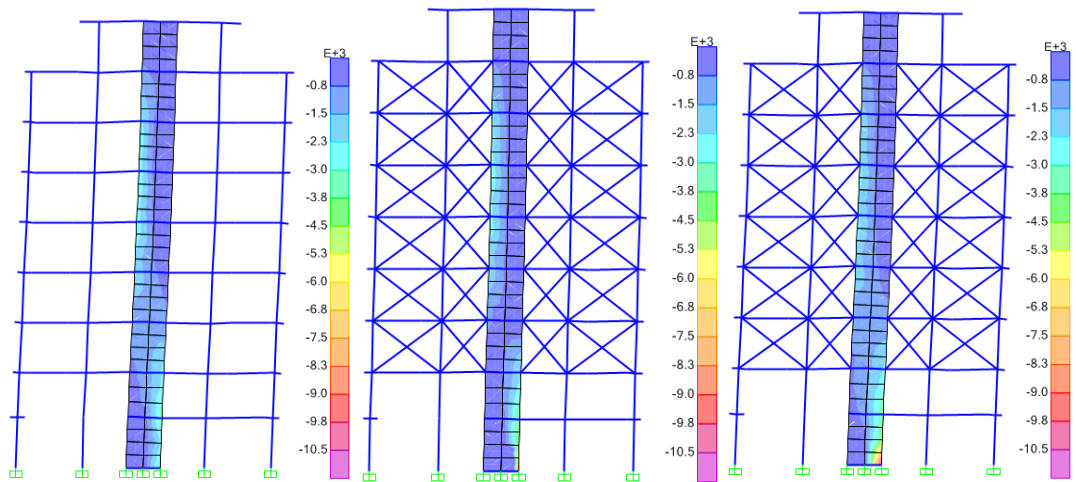
Figure 7.22 Multi Layer Shell Stresses in Reinforcement Layers at the Performance Points According to a) Bare Frame, b) Frame with AAC Infill Wall, c) Frame with Brick Infill Wall, Respectively

As a result of the analyses, when the performance solutions on models and capacity curves are compared, the AAC and brick infill wall frames show similar characteristics. However, the AAC infill wall model has more displacement. When the performance points are investigated, it was observed that brick and AAC infill wall models receive less base shear force and less displacement comparing to bare frame model.

When the shear wall is examined thoroughly, it has been observed that the amounts of concrete compression and tension especially of the brick infill wall model shows a decrease to some extent comparing to the other two models, however it is observed that the steel on base area receives more tension comparing to the other two models.

In the analyses when the influences of the walls are included in the system, it has been observed that the first two modes of brick and AAC wall models have been changed. It is observed that the first mode of bare frame system is the direction of torsion, second mode is x direction and third mode is y direction. However, when the infill wall influence applied to the building systems first and second modes are chanced. First mode is x direction, second mode is the direction of torsion. Third modes are not chanced. Additionally, building height is also important factor for this effect. The period values of the models are provided in Table 7.12.

Table 7.12 Periods of different models

Building Type	T(sec)
Bare frame	0.880
Frame with AAC infill wall	0.658
Frame with brick infill wall	0.589

7.4 Case Study 3

Summary of the building are shown in Table 7.13. The cross sections of the vertical bearing structural elements are constant throughout the height. The ground floor of the building is used as a car park. The sizes of the columns and beams and the slab thickness of the building are summarized in Table 7.14. The existing reinforcement

in the concrete members is provided in Table 7.15. Figure 7.23 shows the floor plans

of the structure and Figure 7.24 shows the partition walls and openings that affect on

the floor beams. The brick wall model and AAC wall model has been shown in

Figure 7.25 and Figure 7.26 as three dimensional, respectively. The building weights

of these different models have been given in Table 7.16.

Table 7.13 Details of the building

Details of Structure	
Date of construction	2004
Function of the building	Apartment
Number of storey	4
Type of concrete	C20
Type of reinforcement	S220
Building height (m)	11.24
Short direction length (m)	15.05
Long direction length (m)	15.70
Floor area (m^2)	236.29
Floor height (m)	Ground Floor: 2.35
	Normal Floor: 3.06
Dynamic and Geotechnical parameters	
Seismic zone coefficient (Ao)	0.2
Allowable bearing pressure (kN/m²)	200.0
Ductility level	High
Horizontal force factor (R)	1.0
Building importance coefficient (I)	1.0
Live load reduction factor (n)	0.3
Spectrum characteristic period (Ta/Tb)	0.15/0.4
Building knowledge level	Medium
Corrosion ratio in the structural elements	0.0
Thermal expansion difference (°C)	0.0
Seismic Code	TDY2007

Table 7.14 Member dimensions of the building

Columns (mm)	650x250, 700x250, 750x250, 800x250, 1250x250
Beams (mm)	250x500
Slab thickness (mm)	200

Table 7.15 Existing reinforcement in members of the building

Columns	Longitudinal Rebars: max. %1.15-min. %1.00 Confinements: Ø8/20/10
Beams	Top Reinforcement: %0.52 Bottom Reinforcement: %0.41 Confinements: Ø8/20/10
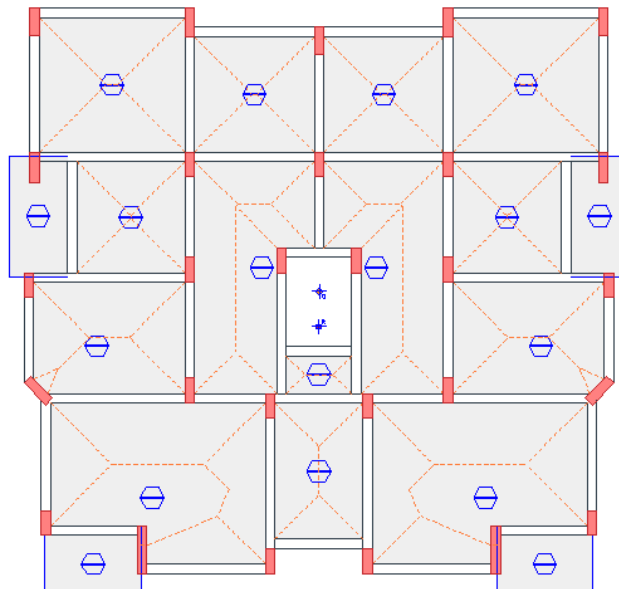
Figure 7.23 Floor Plan of the Building
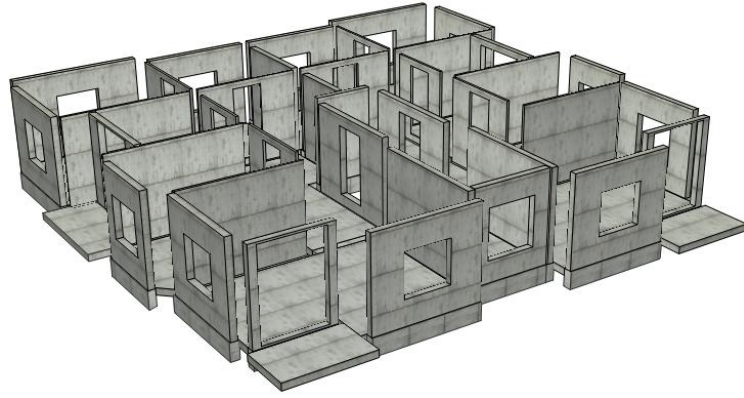
Figure 7.24 3D Locations of Infill Walls on the Beams
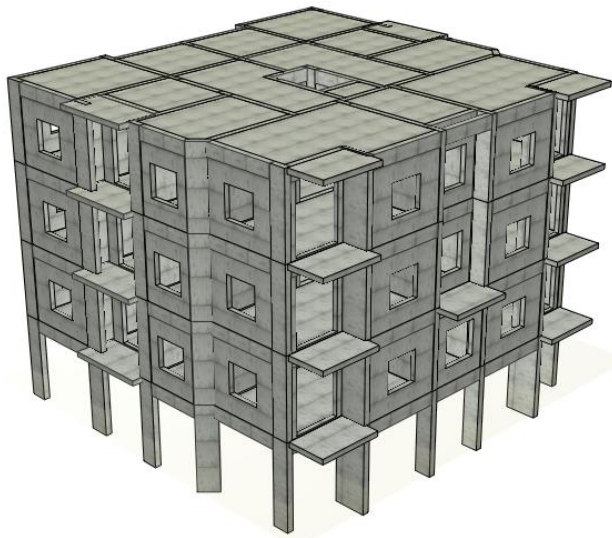
Figure 7.25 3D View of Frame with Brick Infill Wall
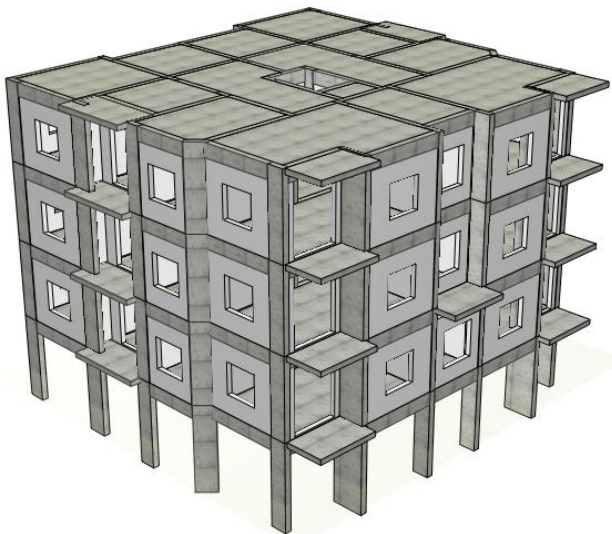
Figure 7.26 3D View of Frame with AAC Infill Wall

Table 7.16 Building weights of different models

Building Type	W(kN)
Bare frame	9487.90
Frame with AAC infill wall	10280.28
Frame with brick infill wall	11018.26

The pushover analyses of different models created for the existing structure have been carried out and the capacity curves have been given in Figure 7.27. Table 7.17 shows the base shear force- displacement values of the performance point obtained by ATC 40. The mechanisms of the performance points for each model have been shown in Figure 7.28, Figure 7.29 and Figure 7.30, respectively.
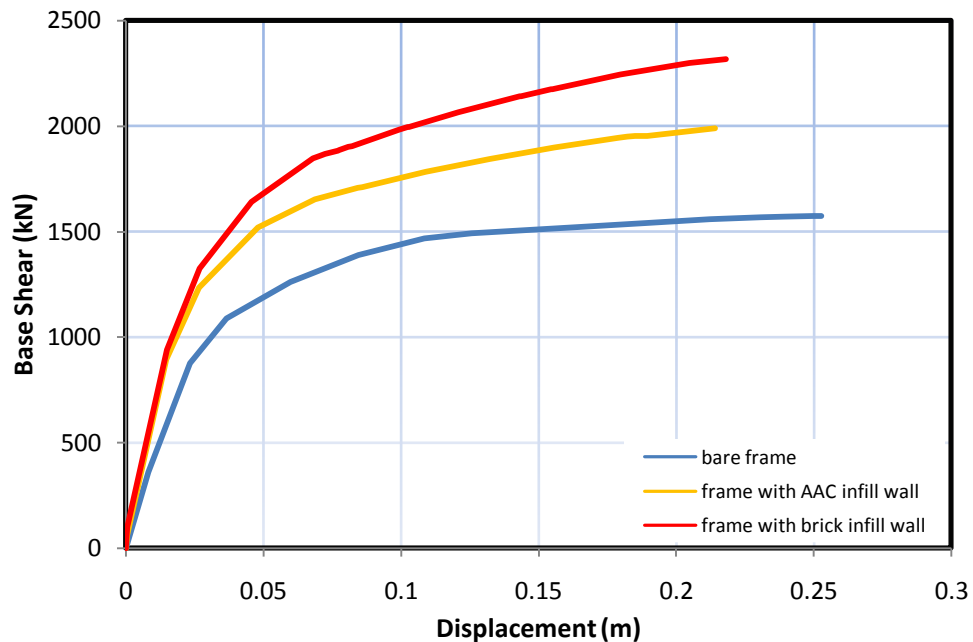
Figure 7.27 Pushover Curves for Case Study 3 utilizing dissimilar Infill Walls Materials

Table 7.17 Performance points for case study 3 using different infill walls material

Building Type	Performance Point		Seismic Performance Level
	Base Shear (kN)	Displacement (m)	
Bare Frame	1199.876	0.052	B-IO
Frame with AAC infill wall	1465.154	0.044	B-IO
Frame with brick infill wall	1680.188	0.05	B-IO
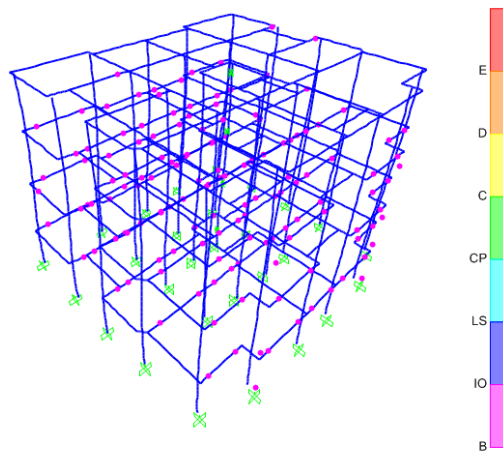
Figure 7.28 Bare Frame Mechanism at the Performance Point
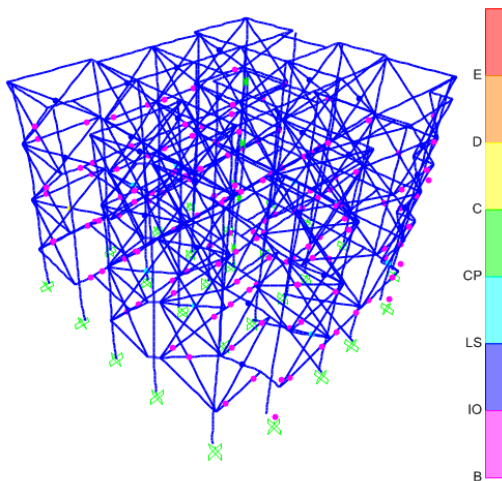
Figure 7.29 Frame with AAC Infill Wall Mechanism at the Performance Point
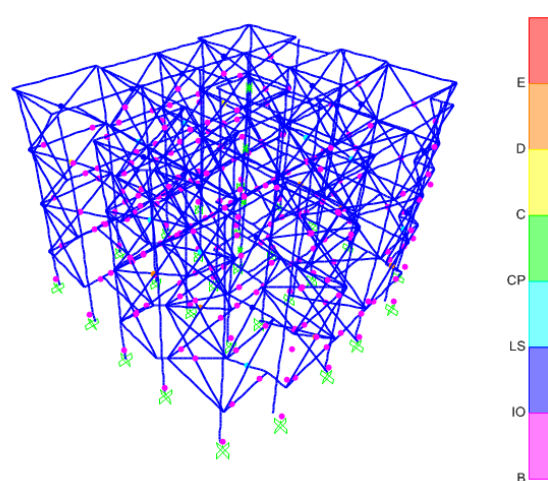
Figure 7.30 Frame with Brick Infill Wall Mechanism at the Performance Point

When the performance curve of the infill wall models are examined, it can be seen that the brick infill wall model receives more base shear force comparing to the other two models and it is more displaced than the AAC infill wall model. However, there was no change in performance levels.

Because the columns are stronger than the beams and the ground floor height is less than the normal floor heights, there has not been a soft story mechanism on the ground floor of the infill wall models. Figure 7.31 and 7.32 shows the failure mechanisms of infill wall frames. Table 7.18 shows the period values of the models.
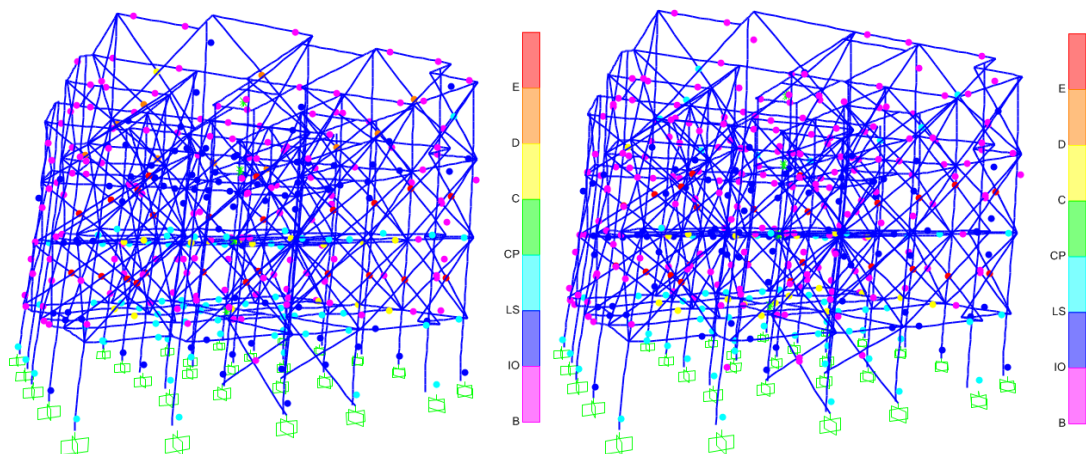
Figure 7.31 Frame with AAC Infill Wall Mechanism at the Collapse Point

Figure 7.32 Frame with Brick Infill Wall Mechanism at the Collapse Point

Table 7.18 Periods of different models

Building Type	T(sec)
Bare frame	0.650
Frame with AAC infill wall	0.398
Frame with brick infill wall	0.347

Chapter 8

CONCLUSION

In this study the influence of masonry infill frame buildings under lateral loads were illustrated through different examples. It is clear that infill walls used for architectural proposes influence the dynamic behavior of the structures. The results of nonlinear pushover analysis show that infill walls carrying portion of the horizontal forces until they reach their carrying capacity and at the same time increase energy absorption capacity of the structure.

Infill walls can provide positive effects in the system with contribution to horizontal stiffness. However, if these infill walls are not positioning properly in the system, they can impose negative effect on the dynamic properties of the structure.

Generally, according to the analysis results, the brick infill wall has shown better performance than AAC infill wall under lateral loads. However, AAC infill walls are lighter than brick infill walls.

Performance analysis shows that large window and door openings are negatively affecting the performance of infill walls. Specifically, large infill wall openings located in the floor plan and also unsymmetrical distribution of infill walls in the plan would cause the torsion effect on the structural system during an earthquake. This also causes the additional forces which are not account in design. It should be

noted that beside the infill wall position on the plans, the geometry of the building is also an important factor for torsion effect.

Additionally, infill walls change the properties of the free vibration on structural system. Infill walls of the structure on the one hand to increase the mass, while the other hand is providing the reduction of the natural vibration period. According to the performance analysis, brick infill walls effect the structural periods significantly according to the bare frame. It decreases the structural period.

The strength of infill wall (E_{infill}) has an important role in comprehensive performance of the structure. The structural response such as roof displacement and structural periods decreases with the increase in E_{infill} value. Moreover, generally, base shear increases with the increase in E_{infill} value. Hence, it is important to choose the right material for infill and consider it in the analysis and design. It is observed that the brick infill walls are generally more effective than AAC infill walls according to roof displacement. It makes less displacement under lateral loads according to the AAC infill walls.

Building behavior varies significantly when the infill walls considering in the structural analysis. After analysis of studies some infill wall models of mode shapes were found dissimilar according to the bare frame model. Therefore, analysis implemented with partition walls which are not modeled in an unconsidered or unrealistic way would not provide correct outcomes. Additionally, building height is also important factor for this effect.

Generally, in critical earthquake regions which will be held of buildings are required to have high ductility. In this way, the energy consisting during an earthquake is damping easier. Additionally, it is economically more desirable for engineers to design high ductile buildings. As high ductile and partition walls placed on the beams as dead load of the structural system, analysis results does not reflect reality. Therefore, the structural behavior factor mentioned from earthquake codes may change.

REFERENCES

Alakoç, C. A., Özcebe, G., & Sucuoğlu, H. (24-25-26 Kasım 1999). Gazbeton Duvarların Davranışı ve Mekanik Özellikleri. *Türkiye İnşaat Mühendisliği XV. Teknik Kongresi*, (pp. 131-146). Ankara.

Altın, S., Ersoy, U., & Tankut, T. (1992). Hysteretic Response of Reinforced Concrete Infilled Frames. *Journal of Structural Engineering. Vol.118, No.8* , pp. 2133-2150.

Asteris, P. G. (2003). Lateral Stiffness of Brick Masonry Infilled Plane Frames. *Journal of Structural Engineering* , ASCE, August 2003.

ATC-40. (1996). Seismic Evaluation and Retrofit of Concrete Buildings. *Applied Technology Council* , Redwood City, CA.

Atkinson, R. H., Noland, J. L., & Abrams, D. P. (1985). A Deformation Failure Theory for Stack - Bond Brick Masonry Prism in Compression. *Proceedings of the 7th International Brick Masonry Conferance.* Vol.1, 577-799.

Baran, M. (2012). Dolgu Duvarların Betonarme Çerçeveli Yapıların Davranışı Üzerindeki Etkilerinin İncelenmesi. *Journal of the Faculty of Engineering and Architecture of Gazi University* , Vol 27, No 2.

Bayülke, N. (2003). Betonarme Yapıların Dolgu duvarları. *Türkiye Mühendislik Haberleri. 4, 426* , 85-98.

Bounopane, S. G., & White, R. N. (1999). Pseudodynamic Testing of Masonry Infilled Reinforced Concrete Frame. *Journal of Structural Engineering. 126(6)* , pp. 578-589.

Brokken, S. T., & Bertero, V. V. (1981). Studies on Effects of Infills in Seismic Resistant R/C Construction. *Report EERC 81-12* , University of California, Berkeley.

Budak, A. (2006). Dolgu Duvarların Yapı Deprem Yükleri Üzerindeki Etkisi. *Yedinci Uluslararası İnşaat Mühendisliğinde Gelişmeler kongresi* . Ekim 11-13- İstanbul.

Celep, Z., & Gençoğlu, M. (2003). Deprem Etkisindeki Betonarme Çerçeve Taşıyıcı Sistem Davranışına Bölme Duvarların Etkisi. *Beşinci Ulusal Deprem Mühendisliği Konferansı.* İstanbul.

Crisafulli, F. J. (1997). Seismic Behaviour of Reinforced Concrete Structures with Masonry Infills. *PhD Thesis* , University of Canterbury, New Zealand.

Crisafulli, F. J., Carr, A. J., & Park, R. (2000). Analytical Modelling of Infilled Frame Structures - A General Overview. *Bulletin of the New Zealand Society for Earthquake Engineering* , Vol.33, No.1.

Decanini, L. D., & Fantin, G. E. (1986). Modelos Simplificados de la Mamposteria Incluida en Porticos. Characteristicas de Rigidez y Resistencia Lateral en Estado Limite. *Jornados Argentinas de Ingenieria Estructural* , Buenos Aires, Argentina, Vol.2, 817-836.

Dowrick, D. J. (1987). *Earthquake Resistant Design for Engineers and Architects.* New York: John Wiley & sons.

Fahjan, Y. M., Başak, K., Kubin, J., & Tan, M. T. (2011). Perdeli Betonarme Yapılar için Doğrusal Olmayan Analiz Metotları. *Yedinci Ulusal Deprem Mühendisliği Konferansı* , İstanbul.

FEMA-356. (2000). Prestandard and Commentary for the Seismic Rehabilitation of Buildings. *Federal Emergency Management Agency* , Washinton D.C.

Grovidan, P., Lakshmipathy, M., & Santhakumar, A. R. (1986, July-August). Ductility of Infilled Frames. *Journal of American Concrete Institute* , pp. 567-576.

Hendry, A. (1981). *Structural Brickwork.* London: Macmillon.

Holmes, M. (1961). Steel Frames with Brickwork and Concrete Infilling. *Proceedings of the Institution of Civil Engineers* , Vol.19, 473-478.

Jadhao, V. P., & Pajgade, P. S. (2013). Influence of Masonry Infill Walls on Seismic Performance of RC Framed Structures a Comparision of AAC and Convertional Brick Infill. *International Journal of Engineering and Advanced Technology (IJEAT)* , ISSN: 2249-8958, Volume-2, Issue-4.

Karslıoğlu, Ö. (2005). Çok katlı Binalarda Bulunan Tuğla Dolgu Duvarların Yapı Davranışına Etkileri. *Yüksek Lisans Tezi* , Kahramanmaraş Sütçü İmam Üniversitesi.

Kızıloğlu, M. Y. (2006). Deprem Etkisi Altında Dolgu Duvarların Betonarme Çerçeve Yapılar Üzerindeki Etkisi. *Yüsek Lisans Tezi* , Yıldız Teknik Üniversitesi.

Klingner, R. E., & Bertero, V. V. (1978). Earthquake Resistance of Infilled Frames. *ASCE Journal of the Structural Division* , Vol.100, 743-757.

Liauw, T. C., & Kwam, K. H. (1984). Nonlinear Behaviour of Non-Integral Infilled Frames. *Computers & structures. Vol.18, No.3* , pp. 551-560.

Mainstone, R. J. (1971). On the Stiffnesses and Strength of Infilled Panels. *Proceedings of the Institution of Civil Engineers* , Supplement IV., 57-90.

Mainstone, R. J., & Weeks, G. A. (1970). The Influence of Bounding Frame on the Racking Stiffness and Strength of Brick Walls. *Proceedings of the 2nd International Brick Masonry Conferance* , Stoke-on-Trent, United Kingdom.

Mander, J. B., Priestley M., J. N., & Park, R. (1988). Theoretical Stress-Strain Model for Confined Concrete. *Journal of Structural Engineering* , Vol. 144, No. 8, pp. 1804-1826.

Mann, W., & Muller, H. (1982). Failure of Shear-Stresses Masonry-An Enlarged Theory, Tests and Application to Shear Walls. *Proceedings of the Seventh International Brick Masonry Conference* , Malbourne, Autralia,Vol.1.

Menegotto, M., & Pinto, P. E. (1973). Method of Analysis for Cyclically Loaded R.C. Plane Frames Including Changes in Geometry and Non-elastic Behaviour of

Elements Under Combined Normal Force and Bending. *Symposium on the Resistance and Ultimate Deformability of Structures Acted on by Well Defined Repeated Loads.* International Association for Bridge and Structural Engineering, Zurich, Switzerland, pp. 139-149.

Merhabi, A. B., Shing, P. B., Schuller, M. P., & Noland, J. L. (1996). Experimental Evaluation of Masonry-Infilled RC Frames. *Journal of Structural Engineering. Asce,122(3)* , pp. 228-237.

Merhabi, A. B., Shring, P. B., Schuller, M. P., & Noland, J. L. (1994). *Performance of Masonry-Infilled R/C Frames Under in-plane Lateral Loads.* Report No. CU/SR-94-6, University of Colorado: Boulder,co.

Negro, P., & Verzeletti, G. (1996). Experimental Evaluation of Masonry Infilled RC Frames. *Journal of Structural Engineering* , p. 228.

Paulay, T., & Priestley, M. (1992). *Seismic Design of Reinforced Concrete and Masonry Buildings.* New York, United States: John Wiles & Sons.

SeismoSoft. (2013). *SeismoStruct-A computer Program for Static and Dynamic Nonlinear Analysis of Framed Structures*. Retrieved from http://www.seismosoft.com/en/SeismoStruct.aspx

Sevil, T. (2010). Seismic Strengthening of Masonry Infilled R/C Frames with Steel Fiber Reinforcement. *P.h.D Thesis* , METU.

Sevil, T., Baran, M., & Canbay, E. (2010, June). Tuğla Dolgu Duvarların B/A Çerçeveli Yapıların Davranışına Etkilerinin İncelenmesi; Deneysel ve Kuramsal Çalışmalar. *International Journal of Engineering Research and Development. Vol.2, No.2* , pp. 35-42.

Smyrou, E. (2006). Implementation and Verification of Masonry Panel Model for Nonlinear Dynamic Analysis of Infilled RC Frames. *Master Thesis* , European School for Advanced studies in Reduction of seismic Risk, Rose School.

Smyrou, E., Blandon-Uribe, C., Antoniou, S., Pinho, R., & Crowley, H. (2006). Implementation and Verification of a Masonry Panel Model for Nonlinear Dynamic Analysis of Infilled Frames. *Proceedings of the First European Conference on Earthquake Engineering and Seismology* , Geneva, 355.

Stafford, S. B. (1962). Lateral Stiffness of Infilled Frames. *Proceedings of the American Society of Civil Engineering, Journal of Structural Division. Vol.88, No.ST6* , pp. 183-199.

Stafford, S. B. (1966). Behaviour of Square Infilled Frames. *Proceedings of the American Society of Civil Engineering, Journal of structural Division. Vol.92, No.ST1* , pp. 381-403.

Varum, H. S. (2003). Seismic Assessment, Strengthening and Repair of Existing Buildings. *PhD Thesis* , University of Aveiro, Portugal.

Wilson, E. L. (2002). *Three Dimensional Static and Dynamic Analysis of Structures.* A Phisical Approach with Emphasis on Earthquake Engineering. Third Edition 2002, Computers and Structures Inc. U.S.A.

Yakut, A., Birinci, B., Demirel, İ. O., & Özcebe, G. (2013). Dolgu Duvarların Deprem Davranışına Etkisi. *2. Türkiye Deprem Mühendisliği ve Sismoloji Konferansı.* 25-27 Eylül 2013-MKÜ-Hatay.

Yıldırım, M. K. (2009). Betonarme Çerçeveli Yapılarda Dolgu Duvar Oranına Göre Yapı Periyodunun Değişiminin Saptanması. *Yüksek Lisans Tezi* , Yıldız Teknik Üniversitesi.

Zhang, B. (2006). Parametric Study on the Influence of Infills on the Displacement Capacity of RC Frames for Earthquake Loss Estimation. *Master Thesis* , European School for Advanced Studies in Reduction of Seismic Risk, Rose School.